



POLITECNICO DI MILANO

Scuola di Ingegneria Civile, Ambientale e Territoriale

PROBABILISTIC SEISMIC HAZARD ANALYSIS
FOR SOUTHEASTERN BRAZIL

Supervisor Prof. Dr. Roberto Paolucci and Dr. Ezio Faccioli

Co-supervisor Sergio Hampshire de Carvalho Santos

Master thesis in Civil Engineering

Thaís De Andrade Ventura

895262

Milan

2021

Abstract of Master of Science thesis presented to Politecnico di Milano as a partial fulfilment of the requirements for the degree of MSc in Civil Engineering

PROBABILISTIC SEISMIC HAZARD ANALYSIS FOR SOUTHEASTERN
BRAZIL

Thaís de Andrade Ventura

April / 2021

Supervisor Prof. Dr. Roberto Paolucci and Dr. Ezio Faccioli

Co-supervisor Sergio Hampshire de Carvalho Santos

The seismic activity of the Brazilian territory is considered very low, however the effects of earthquakes cannot be disregarded in a structural project. The probabilistic analysis method of seismic hazard considers uncertainties and the variability of physical processes that quantify the seismic risk that may affect an entire structure. This work is aimed at determining the response spectrum with return period based on the entire seismological analysis of the Southeastern region of Brazil. A probabilistic analysis is conducted by the R-CRISIS program to generate the response spectrum. This acceleration response spectrum will be applied in a practical example in the structural design of a building under the seismic force and wind force separately, in order to compare the stresses in the structure and, consequently, the structural risk in each situation.

Keywords: Probabilistic analysis; seismic hazard; Southeastern Brazil; CRISIS program.

CONTENTS

1	INTRODUCTION.....	7
1.1	CONTEXT AND MOTIVATION.....	7
1.2	OBJECTIVE OF THE PROJECT	8
1.3	METHODOLOGY	8
2	SEISMOTECTONIC FRAMEWORK OF BRAZIL	10
3	PROBABILISTIC SEISMIC HAZARD ASSESSMENT	19
3.1	EARTHQUAKE CATALOG	19
3.2	SEISMIC SOURCE ZONES AND PARAMETERS	25
3.2.1	SEISMIC SOURCE ZONE MODEL 1.....	31
3.2.2	SEISMIC SOURCE ZONE MODEL 2.....	34
3.2.3	SEISMIC SOURCE ZONE MODEL 3.....	38
3.2.4	ANALYSIS OF G-R RELATIONSHIP FOR THE SEISMIC ZONE MODELS	42
3.3	GROUND MOTION PREDICTION EQUATIONS.....	43
3.4	TREATMENT OF UNCERTAINTIES IN PSHA	47
4	R-CRISIS PROGRAM APPLICATION.....	49
4.1	SOFTWARE INPUT	49
4.2	R-CRISIS ANALYSIS RESULTS.....	56
5	STRUCTURE EXAMPLE APPLICATION.....	60
5.1	PRESENTATION OF THE SPATIAL MODEL	61
5.2	RESULTS ANALYSIS	63
6	CONCLUSIONS	66
	REFERENCES.....	67

LIST OF FIGURES

FIGURE 1 - <i>LOCATION OF ARRAIAL DO CABO IN THE STATE OF RIO DE JANEIRO – BRAZIL</i>	9
FIGURE 2 - <i>MAP OF TECTONIC PLATES . TAKEN FROM FRANCISCO (2018)</i>	11
FIGURE 3 - <i>SOUTH AMERICA SEISMIC HAZARD MAP ACCORDING TO SARA PROJECT. TAKEN FROM SARA.OPENQUAKE.ORG</i>	12
FIGURE 4 - <i>MAP OF BRAZILIAN REGIONS. TAKEN FROM: MAPS-BRAZIL.COM/NORTHERN-BRAZIL-MAP</i>	13
FIGURE 5 - <i>SEISMIC ZONATION OF THE NORTH OF BRAZIL. TAKEN FROM FALCONI (2003)</i>	14
FIGURE 6 - <i>MAPPING OF GROUND CHARACTERISTIC HORIZONTAL PEAK ACCELERATIONS OF BRAZIL FOR EARTHQUAKES ON CLASS B (“ROCK”). TAKEN FROM SANTOS AND SOUZA LIMA (2004)</i>	15
FIGURE 7 - <i>PROBABILISTIC HAZARD MAP FOR ECONOMIC LOSSES IN SOUTH AMERICA DUE TO EARTHQUAKES .TAKEN FROM JAISWAL ET AL (2014)</i>	16
FIGURE 8 - <i>PROBABILISTIC HAZARD MAP FOR LIFE LOSSES IN SOUTH AMERICA DUE TO EARTHQUAKES .TAKEN FROM JAISWAL ET AL (2014)</i>	17
FIGURE 9 - <i>IDENTIFICATION OF THE COMPLETENESS PERIOD FOR CLASS OF MAGNITUDE ≥ 3</i>	21
FIGURE 10 - <i>IDENTIFICATION OF THE COMPLETENESS PERIOD FOR CLASS OF MAGNITUDE ≥ 3.521</i>	
FIGURE 11 - <i>IDENTIFICATION OF THE COMPLETENESS PERIOD FOR CLASS OF MAGNITUDE ≥ 4.022</i>	
FIGURE 12 - <i>IDENTIFICATION OF THE COMPLETENESS PERIOD FOR CLASS OF MAGNITUDE ≥ 4.522</i>	
FIGURE 13 - <i>IDENTIFICATION OF THE COMPLETENESS PERIOD FOR CLASS OF MAGNITUDE ≥ 5.023</i>	
FIGURE 14 - <i>IDENTIFICATION OF THE COMPLETENESS PERIOD FOR CLASS OF MAGNITUDE ≥ 5.523</i>	
FIGURE 15 - <i>IDENTIFICATION OF THE COMPLETENESS PERIOD FOR CLASS OF MAGNITUDE ≥ 6.024</i>	
FIGURE 16 - <i>EARTHQUAKES EVENTS OF SOUTHEASTERN BRAZIL FROM WORKING CATALOG. SITE OF ARRAIAL DO CABO CITY MARKED ON THE MAP WITH A STAR</i>	26
FIGURE 17 - <i>SEISMIC SOURCE ZONE 1A</i>	31
FIGURE 18 - <i>GR RELATIONSHIP TO SEISMIC ZONE (1A)</i>	33
FIGURE 19 - <i>SEISMIC SOURCE ZONE MODEL 2: CONTINENTAL PORTION , SEISMIC ZONE (2A)</i>	34
FIGURE 20 - <i>SEISMIC SOURCE ZONE MODEL 2: CONTINENTAL SHELF, ZONE (2B)</i>	35
FIGURE 21 - <i>GR RELATIONSHIP OF SEISMIC SOURCE ZONE MODEL 2- (2A) : CONTINENTAL PORTION</i>	36
FIGURE 22 - <i>GR RELATIONSHIP OF SEISMIC SOURCE ZONE MODEL 2 – (2B): CONTINENTAL SHELF</i>	37
FIGURE 23 - <i>REPRESENTATION OF SEISMIC ZONES OF MODEL 3 - THE CONTINENTAL PORTION WHICH ARE ZONES (3A) AND (3B), GREEN AND BLACK AREAS, RESPECTIVELY</i>	38

FIGURE 24 - GR RELATIONSHIP OF SEISMIC SOURCE ZONES MODEL 3 – (3A) : INCLUDING.....	39
FIGURE 25 - GR RELATIONSHIP OF SEISMIC SOURCE ZONES MODEL 3- (3B) : INCLUDING PART OF SÃO PAULO,	40
FIGURE 26 - SEISMIC SOURCE ZONE CASE MODEL 3 – (3C) : CONTINENTAL SHELF	41
FIGURE 27 - DEFINITION OF THE DISTANCE METRICS USUALLY USED IN THE GMPEs. TAKEN FROM ILYA SIANKO ET. AL, 2019, A PRACTICAL PROBABILISTIC EARTHQUAKE HAZARD ANALYSIS TOOL: CASE STUDY MARMARA REGION.....	43
FIGURE 28 - GROUND MOTION PARAMETERS LOGNORMALLY DISTRIBUTED.	44
FIGURE 29 - GMPE ERROR NORMAL DISTRIBUTION AND DEVIATION STANDARD. TAKEN FROM ENGINEERING SEISMOLOGY COURSE SLIDES, POLITECNICO DI MILANO,2018.....	45
FIGURE 30 - LOGIC TREE FOR THE GMPEs CHOSEN AND EACH SEISMIC ZONE MODEL.	48
FIGURE 31 - SOURCE ZONE GEOMETRY DATA AS R-CRISIS INPUT FOR THE SEISMIC SOURCE ZONE 1A	50
FIGURE 32 - SEISMICITY DATA INPUT RELATED TO THE SEISMIC SOURCE ZONE MODEL 1A.....	51
FIGURE 33 - ATTENUATION MODEL SELECTION FOR R-CRISIS INPUT	52
FIGURE 34 - ATTENUATION DATA INPUT OF R-CRISIS SOFTWARE	53
FIGURE 35 - INTENSITIES FOR EACH SPECTRAL ORDINATE FOR R-CRISIS INPUT	54
FIGURE 36 - GLOBAL PARAMETERS FOR THE PSHA ANALYSIS.....	55
FIGURE 37 - SEISMIC HAZARD MAP FOR SEISMIC SOURCE ZONE MODEL 1 USING TORO ET AL. (1997) GMPE.....	56
FIGURE 38 - SEISMIC HAZARD MAP FOR SEISMIC SOURCE ZONE MODEL 2 USING ATKINSON AND BOORE (2006) GMPE.....	57
FIGURE 39 - SEISMIC HAZARD MAP FOR SEISMIC SOURCE ZONE MODEL 3 USING ATKINSON AND BOORE (2006) GMPE.....	57
FIGURE 40 - 50-YEARS EXCEEDANCE RATE CURVES FOR $T=0.01s$ SA SPECTRUM ORDINATES CONTRIBUTED BY DIFFERENT SEISMIC SOURCE ZONE MODELS AND GMPEs	58
FIGURE 41 - UNIFORM HAZARD ACCELERATION RESPONSE SPECTRA FOR 0.10-IN-50 YEAR EXCEEDANCE PROBABILITY FOR EACH SEISMIC SOURCE MODEL AND GMPEs SELECTED ..	59
FIGURE 42 - 3D MODEL OF THE CONCRETE BUILDING IN ROBOT SOFTWARE	61
FIGURE 43 – PLAN OF THE FIFTH STOREY OF THE BUILDING	62
FIGURE 44 - ACCELERATION RESPONSE SPECTRUM FOR 475 YEARS (LEFT); ACCELERATION RESPONSE SPECTRUM FOR 2475 YEARS (RIGHT).....	63
FIGURE 45 - DISPLACEMENTS ALONG THE HEIGHT OF THE BUILDING IN Y DIRECTION	64

1 INTRODUCTION

1.1 CONTEXT AND MOTIVATION

Although earthquakes can be generated by volcanic eruptions and explosions, the most common cause by far is the relative movements between tectonic plates. The energy released at the source of the earthquake spreads through rock and soil. The disasters caused by an earthquake can be severe, an entire structure can be damaged and many people can die. In our history there have been many seismic events that caused vast losses to humanity.

Earthquakes with less than 5.0 degrees magnitude on Richter scale are generally not capable of causing structural damage to modern construction. From this value, the structures can be damaged easier. Brazil is known to be “free” from earthquakes as it is a country located in the center of a tectonic plate. However, there are recorded events with more than 6.0 Richter magnitude, one in 1955 with magnitude 6.6 in Mato Grosso and another one in 1955 with magnitude 6.3 in Espírito Santo, both in southeastern Brazil. When those earthquakes happened, the areas were not inhabited, but nowadays these are regions with well-developed cities, huge infrastructure and nuclear power plants. That is the reason why seismic hazard analysis has been developed in the past years in Brazil.

Probabilistic methods are used for seismic hazard because there is a real difficulty in obtaining a sufficient number of events to establish a representative database for this kind of natural events. The objective of a probabilistic seismic hazard analysis (PSHA) is to provide a long-term overview of the relationships between ground motion levels and their occurrence frequencies. In this framework, the ground motion prediction equations play an important role in this research, as they are used by programs to compute the response spectrum at a site with a given return period.

Besides the methods to predict a seismic event and its ground acceleration, it is important to know how reliable a structure in southeastern Brazil is when a dynamic force is applied, the ground motion acceleration. The structural analysis for residential or commercial buildings in Brazil are carried out nowadays considering only static forces, commonly the wind force. In order to compare the stresses caused in a practical building example, two analysis will be generated under its self-weight and two types of loadings, a dynamic one and static one.

1.2 OBJECTIVE OF THE PROJECT

The objective of this work is to generate probabilistic response spectra for the reference site and make a structural analysis comparing the stresses of a building under a dynamic force caused by a seismic event and under a static force caused by the wind. The first step is the computation of the data necessary for R-CRISIS program input. The seismic catalog of the southeastern Brazil is from the year of 1724 until 2016 and it is the main source for this data computation. The output of the probabilistic seismic hazard analysis is the acceleration response spectrum which will be applied to a theoretical building.

The structural analysis will be conducted considering the seismic dynamic loading and the wind static loading separately, in order to compare the stresses caused by each type of loading in the building. This comparison is important to show the risk between structural analysis in Brazil considering only wind forces and the possibility to consider also seismic events as a dynamic force.

1.3 METHODOLOGY

The objective of a probabilistic seismic hazard analysis (PSHA) is to provide a long-term assesment of the relationships between ground motion levels and their occurrence frequencies. A PSHA allows the user to obtain feasible earthquakes with different locations, magnitudes, and occurrence frequencies, associated to all the seismic sources of interest. For this case, the PSHA was developed using the latest version of the program R-CRISIS, a well-known and accepted tool that implements state-of-the-art methodologies to perform PSHA (Ordaz et al., 2013).

To fulfil the project objective, the first step of this work has as reference the research done by Santos and Lima (2008) , Dourado (2013) and Romero et tal. (2013). All of them have already done a probabilistic seismic hazard in some regions of Brazil but using the ground motion prediction equations in different ways.

From these references, the data of seismic events that occurred in southeastern Brazil was analyzed and computations were done in order to get the final parameters for the seismic hazard analysis. The location site used as reference is the city of Arraial do Cabo – RJ. The

computer program R-CRISIS allows to choose a ground motion prediction equation to compute de acceleration response spectrum. In this study, Toro et. al. (1997) and Atkinson and Boore (2003) were the GMPEs used.

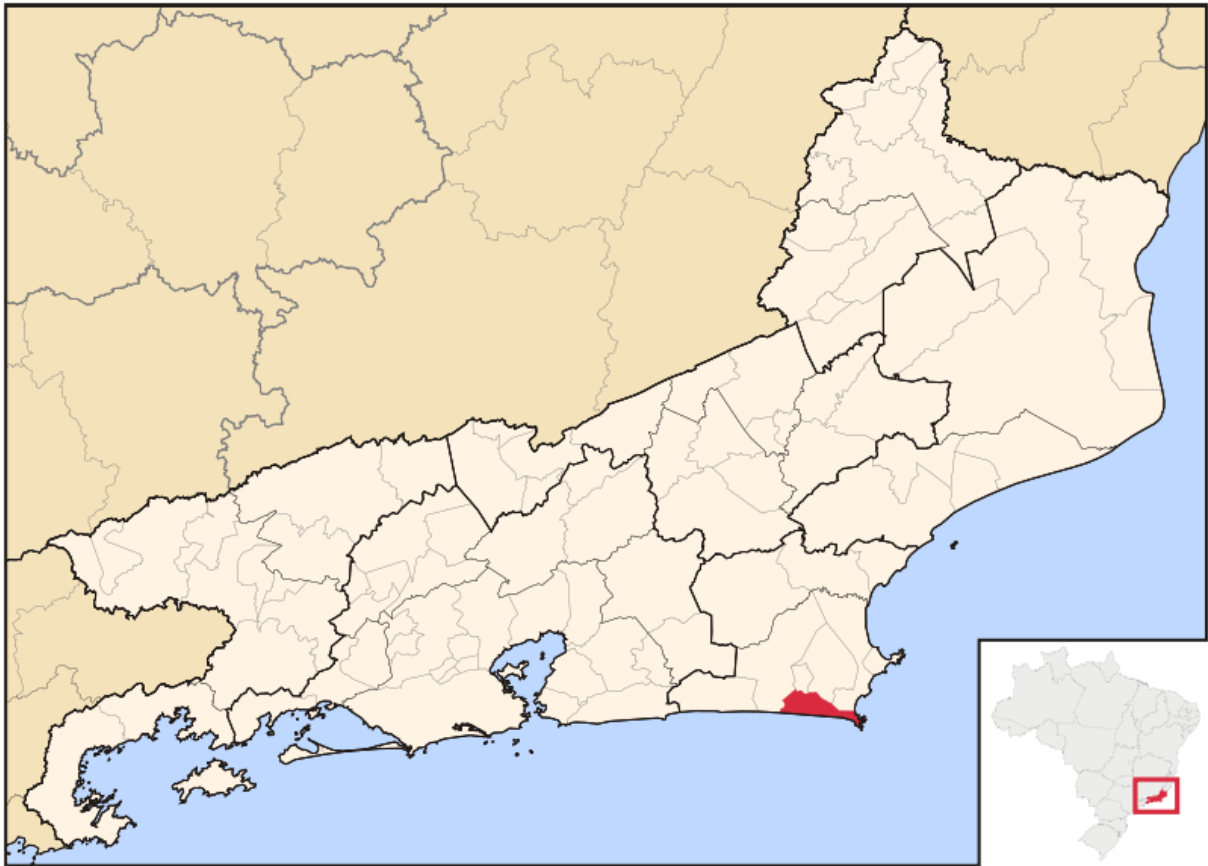


Figure 1 - Location of Arraial do Cabo in the state of Rio de Janeiro – Brazil.

Taken from MesoMicroMunicip.svg

Consequently, the peak ground acceleration for the specific site was found with the generated acceleration response spectrum. The next step was to apply this acceleration to a theoretical concrete building of 8 storey as a dynamic loading. The first structural analysis consists of getting the stresses of a central column caused by the self-weight and the seismic acceleration with return periods of 475 years and 2475 years. A second structural analysis will be carried out considering only the self-weight of the building and the wind force, as a static loading. In Brazil is not common to consider seismic dynamic forces in residential or commercial buildings, therefore the goal of these two analyses is to compare the stresses found for each loading situation and discuss the critical scenario that may happen with a potential seismic event occurrence.

2 SEISMOTECTONIC FRAMEWORK OF BRAZIL

The regions on Earth where the largest earthquakes occur, i.e. the most seismically active regions, coincide with the limits of tectonic plates. The edge of oceanic and continental plates is where over 90% of the world earthquakes occur. Plate boundary regions have the seismicity relatively concentrated and earthquakes causes are well understood, however intraplate seismicity represents diffuse deformation in relatively stable tectonic regions, and its origins cannot be explained simply, given that they depend on the local tectonic context. Brazil seismic scenario is included in these intraplate seismicity cases.

The studies of Assumpção et al. (2004) based on seismic tomography results show that lithospheric thinning could provide favorable conditions for stress concentration in the brittle upper crust, which may explain the epicentral distribution within the South American Platform. In regions of tectonic lithospheric thinning, the stress tends to focus on the crust, while in regions of thicker lithosphere the stress is more distributed within the upper mantle.

Seismological research in South America started to be developed at the end of XIX century, with the installation of the Observatório Nacional station at Rio de Janeiro. From 1977 to 1992, Observatório Nacional accumulated a valuable data set of long period analog records, which have been used to investigate crustal and upper mantle structure of Brazil by surface wave dispersion (Souza , 1988; 1991). In Brazil, information about crustal thickness is limited and concentrated in some regions of the country. According to Assumpção et al. (1997), crustal thickness in southeastern Brazil varies from 37 to 47km



Figure 2 - Map of Tectonic Plates . Taken from Francisco (2018)

In fact, comparing Brazil to other regions of the planet, or even to South America, we can see that its seismic activity is less, and it is relatively low. For this reason, there is no great interest in the development of seismic research in this region, as there is in the regions of high level of seismic activity. Even so, in recent times, information has been compiled on earthquakes that have occurred since historical times in Brazil.

There is not yet a complete analysis of the seismicity of the Brazilian territory. There is, however, a study of seismic risk in South America as a Global Earthquake Model initiative which lasted between 2013 and 2015. The South America Risk Assessment (SARA) project “ aimed to calculate hazard and risk, and to estimate the compounding social and economic factors that increase the physical damage and decrease the post-event capacities of populations to respond to and recover from damaging earthquake events in South America, by involving local experts from throughout the region” (sara.openquake.org). Figure 3 shows the seismic hazard map related to the peak ground acceleration with exceedance of 10% in 50 years.

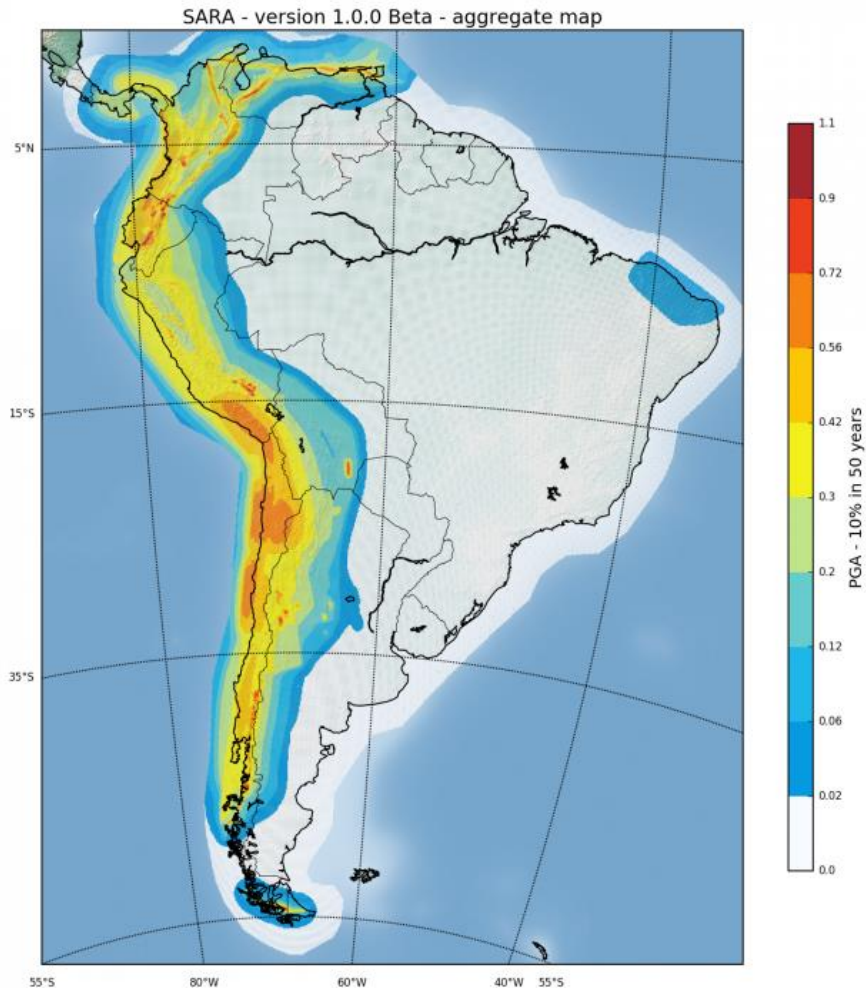


Figure 3 - South America seismic hazard map according to SARA project. Taken from sara.openquake.org

It is notable, in this map, that the Brazilian territory presents low seismicity, with ground horizontal peak accelerations usually under $0.04g$ or $0.4m/s^2$. It is worth also mentioning that in some areas of Brazil seismicity is not negligible. The regions with higher seismicity are some states of the Northeast, due to its position in relation to the tectonic fault of the Central Atlantic, and in the North part, Acre and Amazonas states, due to its proximity to the Andes Mountains. Figure 4 demonstrates the regions of Brazil in order to clarify the states that have been mentioned in this text.



Figure 4 - Map of Brazilian regions. Taken from: maps-brazil.com/northern-brazil-map

A research done by Falconi (2003) presents a comparative analysis between seismic projects normalizations of 6 countries of South America. Brazil was not included in this research, but the presented seismicity specially in the North of the country, especially the region of Acre and Amazonas states, can be inferred using zoning data from neighboring countries. Figure 5 above shows this zonation.

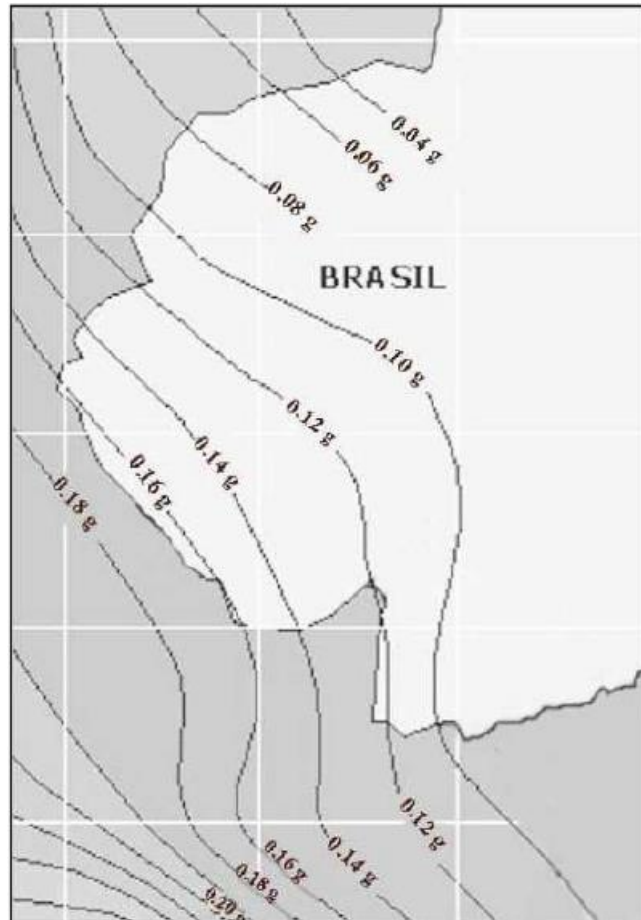


Figure 5 - Seismic zonation of the North of Brazil. Taken from Falconi (2003)

Considering this research and taking into account the geographic continuity between neighboring countries, the seismicity map of South America was consolidated by Santos and Souza Lima (2004). These same analysis were used to define the seismic zones to Brazil presented in the Brazilian Earthquakes Standard (NBR 15421).

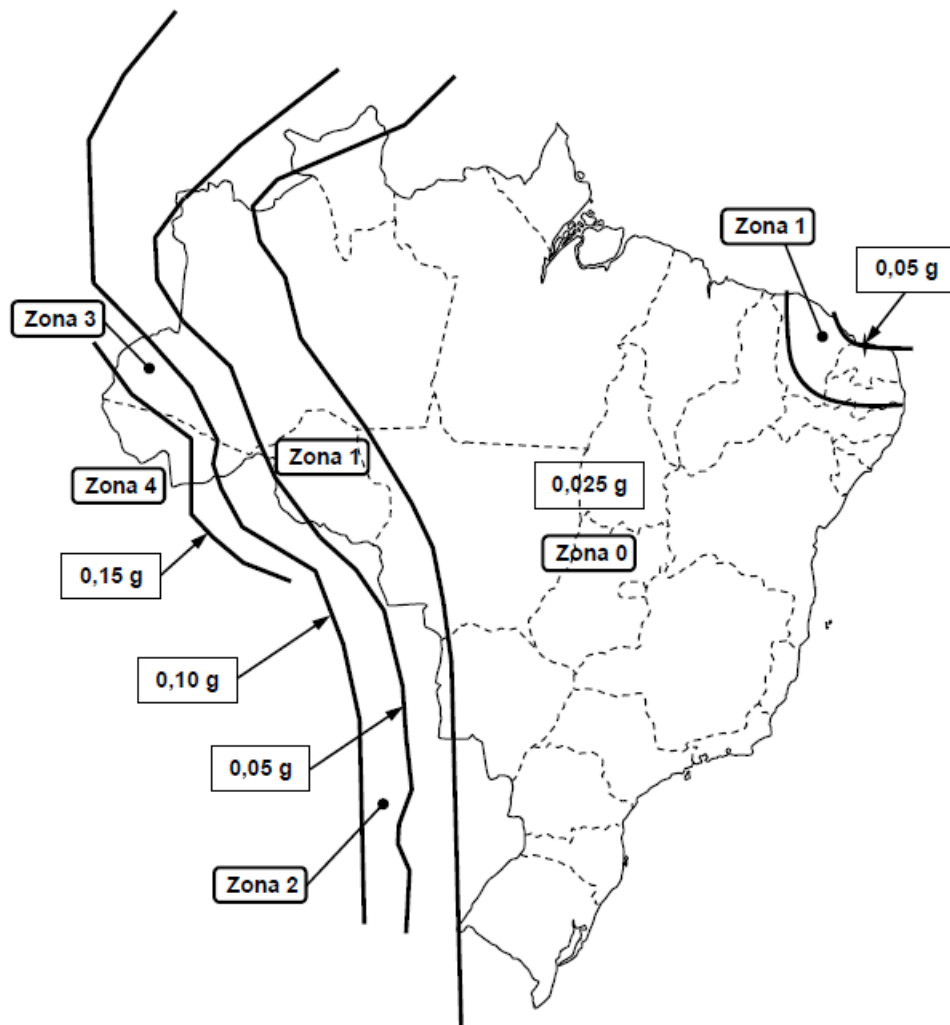


Figure 6 - Mapping of ground characteristic horizontal peak accelerations of Brazil for earthquakes on class B ("rock"). Taken from Santos and Souza Lima (2004)

The Brazilian Earthquake Standard, NBR 15421 (2006) takes into account the higher seismicity of these regions, highlighting greater probability of earthquakes occurring in them. The NBR 15421 divides the Brazilian territory into zones, considering the return period of 475 years, it means the probability of exceedance 10% in 50 years. The first is Zone 0 which has the characteristic acceleration for soil Class B (rock) of 0.025g and the last one is Zone 4 with characteristic acceleration of 0.15g.

It is notable the Brazilian territory is not free from earthquakes. Though the biggest frequency of earthquakes be at the interface between tectonic plates, earthquakes can occur anywhere in Brazil (which characterizes diffuse seismicity). Because of that, there are records of earthquakes in regions that are not in principle subject to earthquakes.

Although the Brazilian Southeast region is not one of the most seismic, it should receive special attention, because it is a highly populated region with a well-developed infrastructure.

Considering the risk aspect, Jaiswal et al. (2014) sought to quantify South America's seismic risk in terms of life risk and economic losses. Figures 7 and 8 present the risk in terms of economic losses and loss of life.

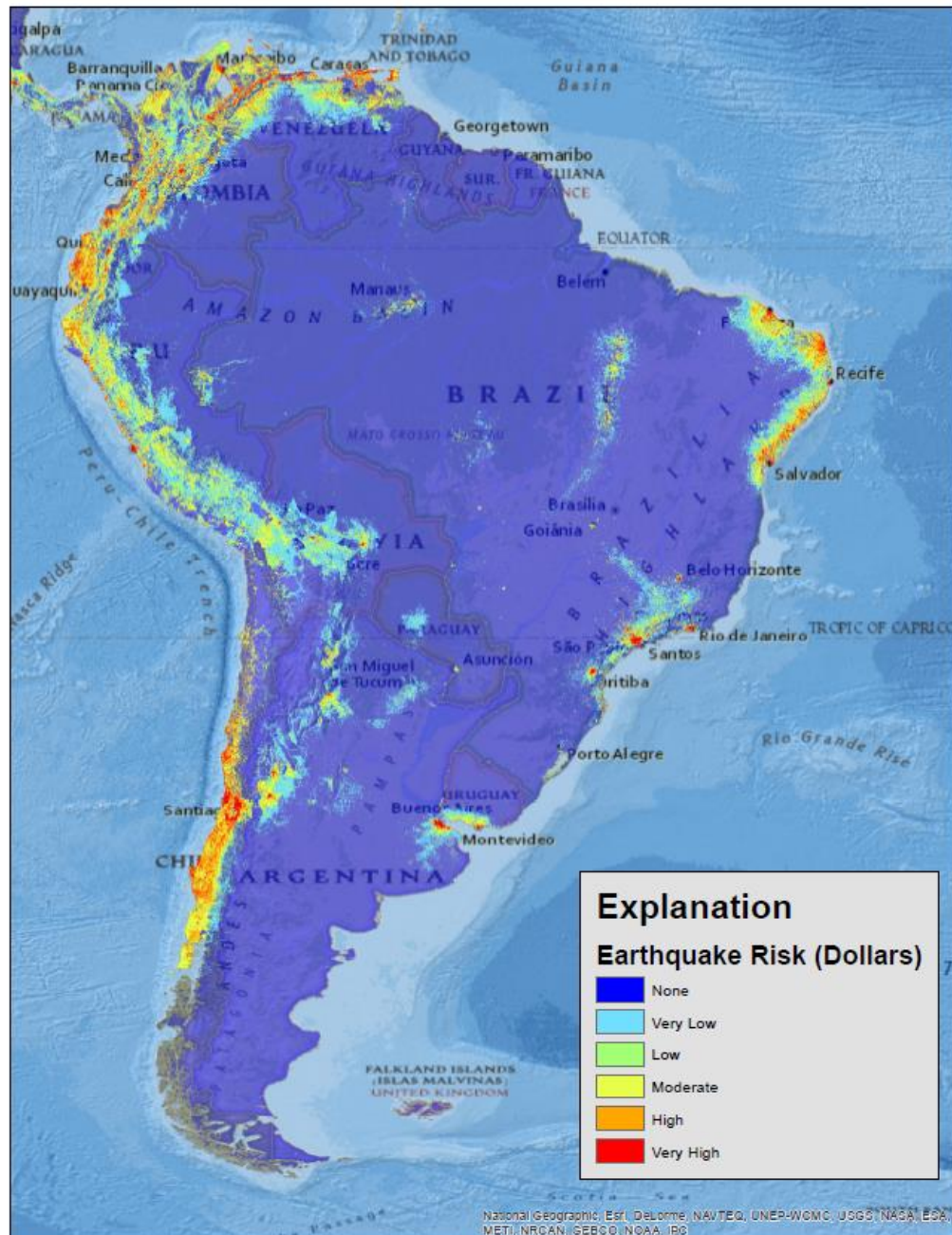


Figure 7 - Probabilistic hazard map for economic losses in South America due to earthquakes .Taken from Jaiswal et al (2014).



Figure 8 - Probabilistic hazard map for life losses in South America due to earthquakes .Taken from Jaiswal et al (2014).

It can then be observed that regions such as the Brazilian Southeast have a greater risk. This region has the risks from moderate to very high based on the map colors, both at risk of economic loss and of lives, which are higher than the Acre state with risks from none to very low, which is more exposed to strong earthquakes. A possible earthquake in the Southeast,

even if less pronounced, can generate greater losses than one in less developed and inhabited regions.

The Brazilian region that contains the most data collected is the Southeast. This is because the region has several monitoring systems, on oil platforms, and in hydroelectric and nuclear power plants. Since most seismological studies are probabilistic, the more data available, the more accurate the analyses are likely to be. This thesis study will illustrate the probabilistic seismic hazard analysis with CRISIS program based on the Brazilian seismic catalog and data available for Southeast region.

3 PROBABILISTIC SEISMIC HAZARD ASSESSMENT

The seismic hazard assessment developed in this study follows a probabilistic approach, as formulated by Cornell (1968), that estimates the probabilities of exceedance of given levels of ground motion over a specific time frame and allows to properly take into account the uncertainties related to the determination of the location and magnitude of the earthquake, the process of occurrence of seismic events and the attenuation characteristics of the seismic motion. The computer code R-CRISIS, Ordaz et al. (1991), chosen to perform the hazard calculations for this study, uses Bayesian models of hazard analysis (Morgat and Shah, 1979), and treats as random variables the regional seismicity parameters and the maximum magnitude.

The inputs of the calculation include: (1) a seismic catalog that covers 292 years, homogenized to moment magnitude M_w and completeness periods discretization; (2) an area-source model containing seismogenic zones, which are characterized with corresponding seismic parameters; and (3) ground-motion prediction equations (GMPEs), which have been identified from amongst existing models better able to reproduce the attenuation of the country. In addition, a simple logic tree is formulated in order to consider the epistemic uncertainty related with GMPEs. These aspects will be discussed in detail in the following sections.

3.1 EARTHQUAKE CATALOG

A primary component of the PSHA model is the earthquake catalogue for the region. The seismic catalogue of this work contains records from 1724 to December 2016. It includes historic information published in specific studies and by different agencies. The principal source is the seismic catalog of the Brazilian Seismic Bulletin (BSB) that is elaborated by the Institute of Astronomy, Geophysics and Atmospheric Sciences of the University of São Paulo (IAG-USP). These official agencies directly give the moment magnitude scale, M_w , estimated from the empirical global correlation with the body wave magnitude, M_b .

$$M_w = [0.84 (\pm 0.04) \times M_b] + 1.03 (\pm 0.23) \quad (1)$$

The assembled working catalog has been ordered and thoroughly checked to exclude induced earthquakes and aftershocks. The final catalogue has 2124 epicenters in the Brazilian territory of earthquakes of magnitudes 2,7 to 6,3 occurred from 1724 to 2016. At this part of this study, the referred working catalog takes into account the seismic events around the whole territory of the country and not only on the Southeastern region, because, compared to other seismic active countries, Brazil does not have a great number of earthquake events and the results of the completeness steps become more reliable when considering all the events occurred since the year 1724.

In order to continue the completeness of the working catalog, a visual-cumulative method is used and the earthquakes are grouped within classes of magnitude greater or equal to 3,0. The chosen classes of magnitude are based on the PSHA study done by Berrocal et al (2013), and their cumulative number of events are shown in Table 1.

M Classes	Cumulative Numbers
$M \geq 3.0$	1617
$M \geq 3.5$	924
$M \geq 4.0$	429
$M \geq 4.5$	107
$M \geq 5.0$	50
$M \geq 5.5$	14
$M \geq 6.0$	2

Table 1 - *Number of cumulative earthquake events of each class of magnitude*

For each class of magnitude, the cumulative number of earthquakes is plotted as a function of time with a time interval of 50 years. The most recent periods of time have the cumulative number well approximated by a straight line and the changes of trend in the cumulative number of earthquakes identifies the periods of completeness. It is a practical but reliable method to find the completeness periods since the older is the catalog data, the scarcer and more uncertain the news about seismic events become. The following figures show the plots of cumulative number of earthquakes vs interval of time and the final definition of the completeness periods on Table 2.

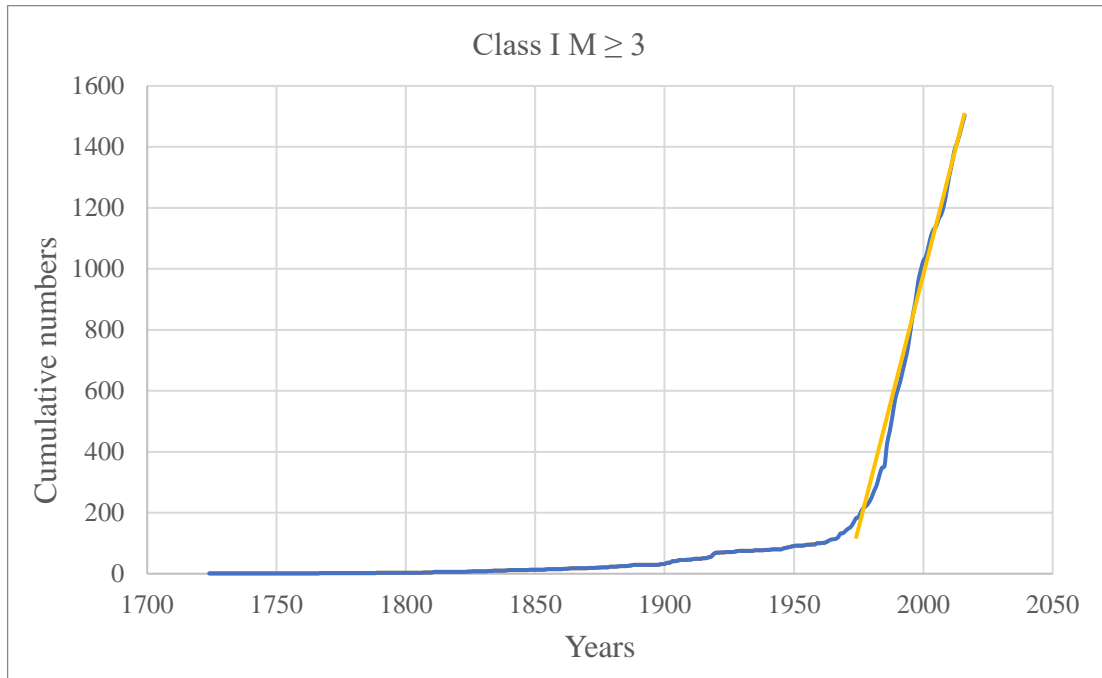


Figure 9 - Identification of the completeness period for class of magnitude $\geq 3,0$

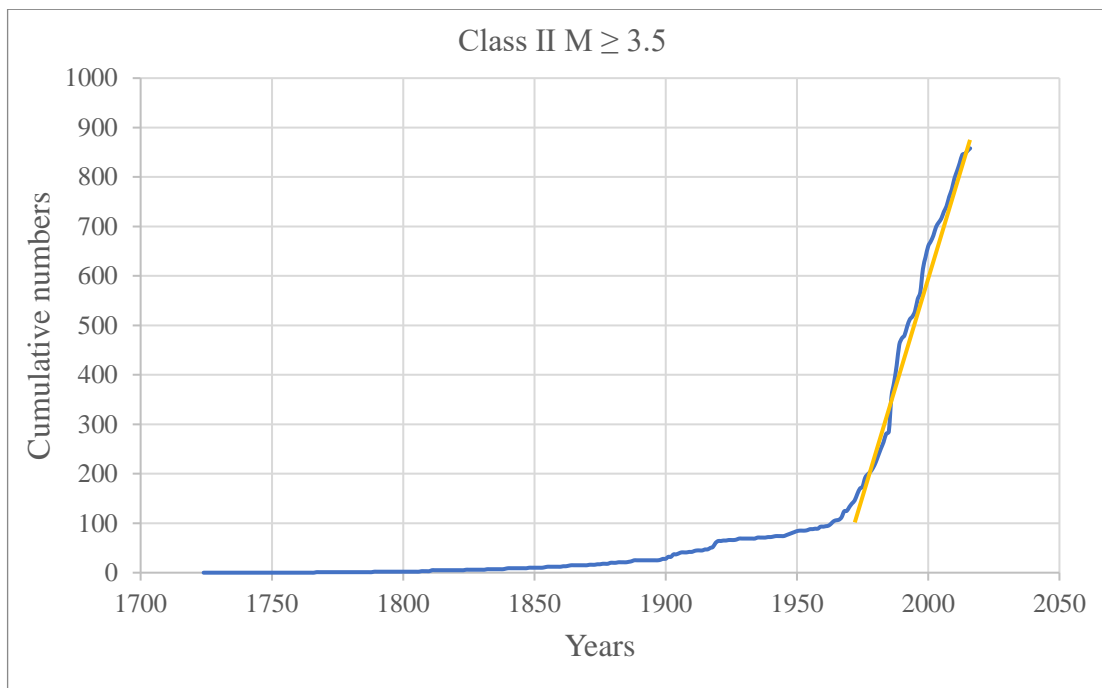


Figure 10 - Identification of the completeness period for class of magnitude $\geq 3,5$

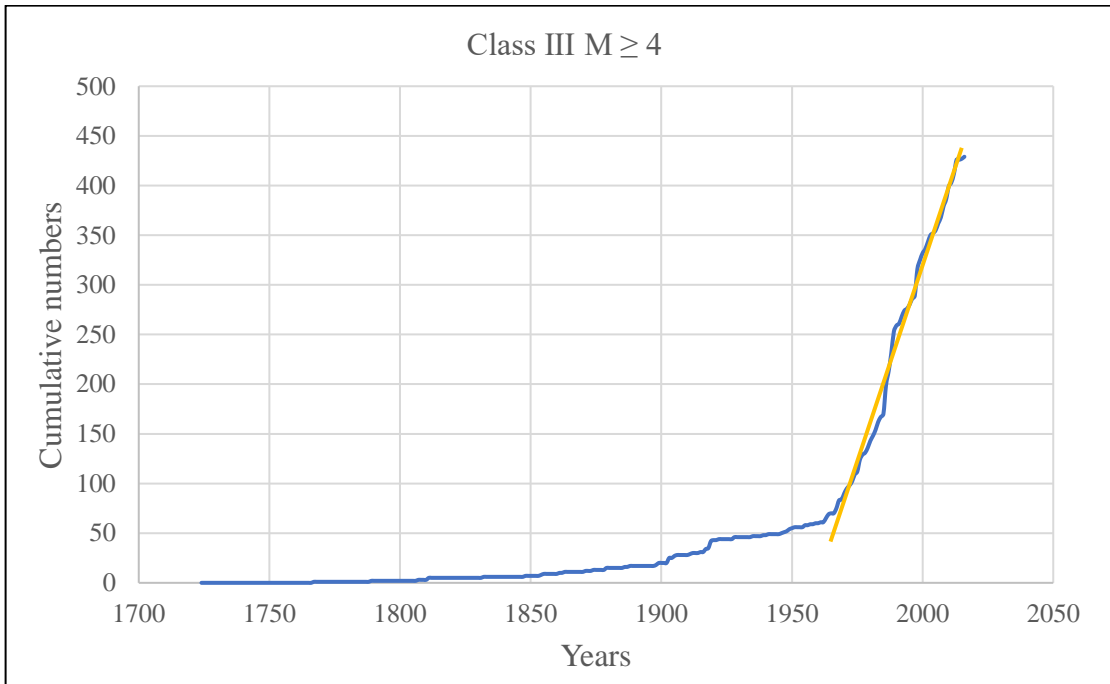


Figure 11 - Identification of the completeness period for class of magnitude $\geq 4,0$

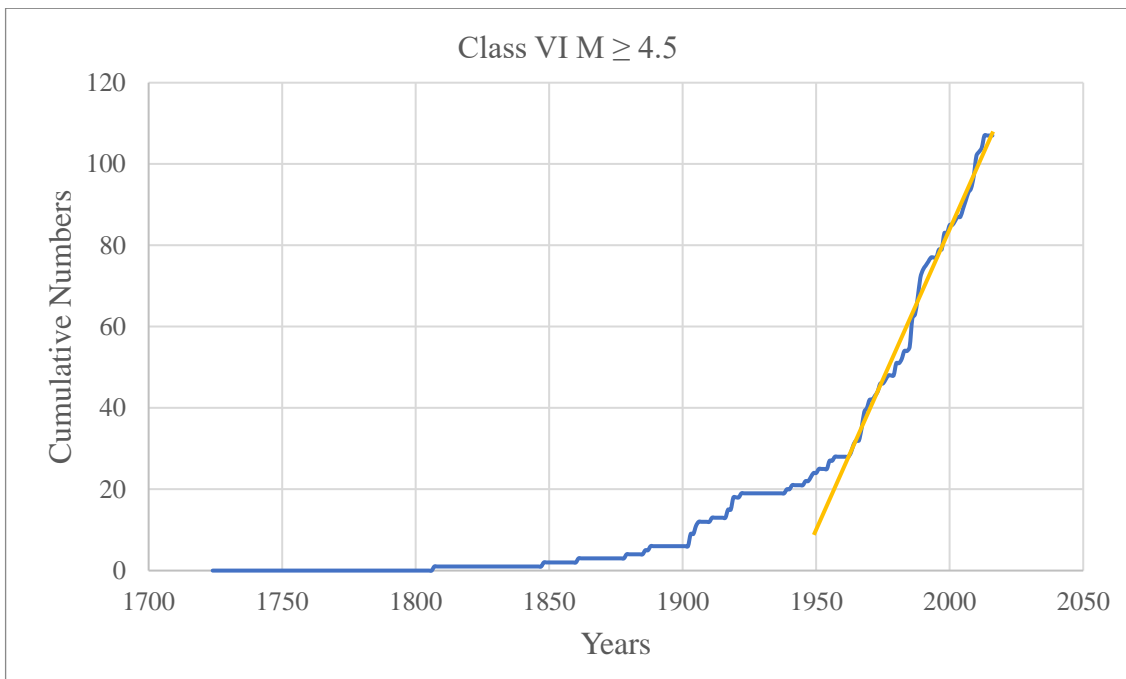


Figure 12 - Identification of the completeness period for class of magnitude $\geq 4,5$

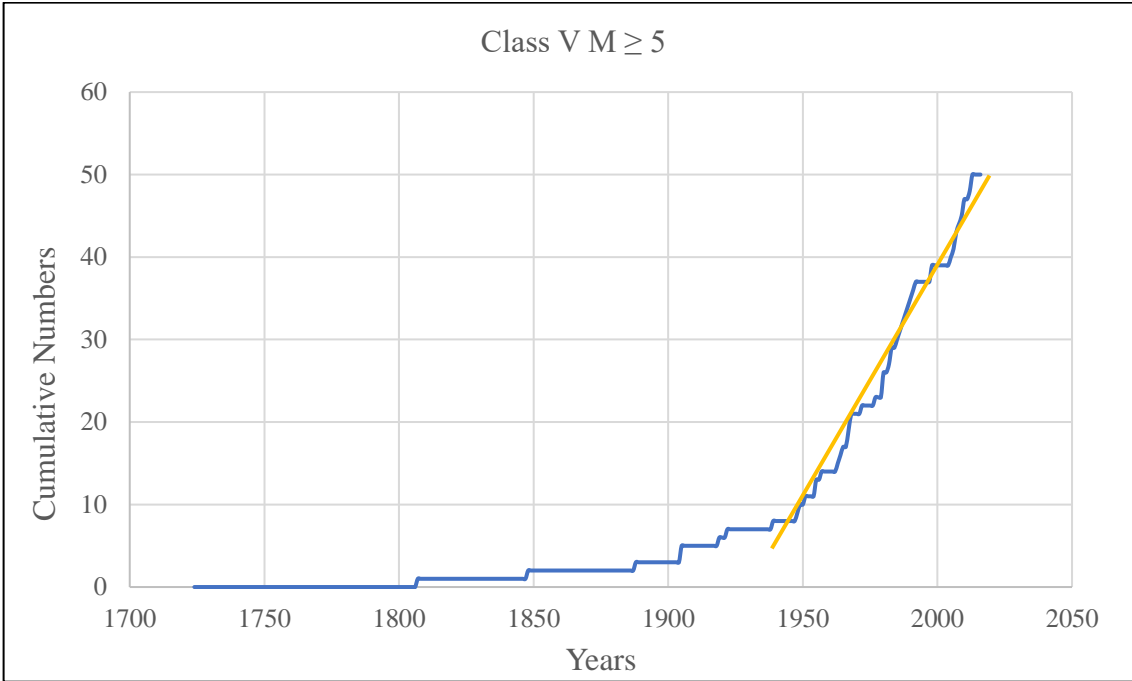


Figure 13 - Identification of the completeness period for class of magnitude $\geq 5,0$

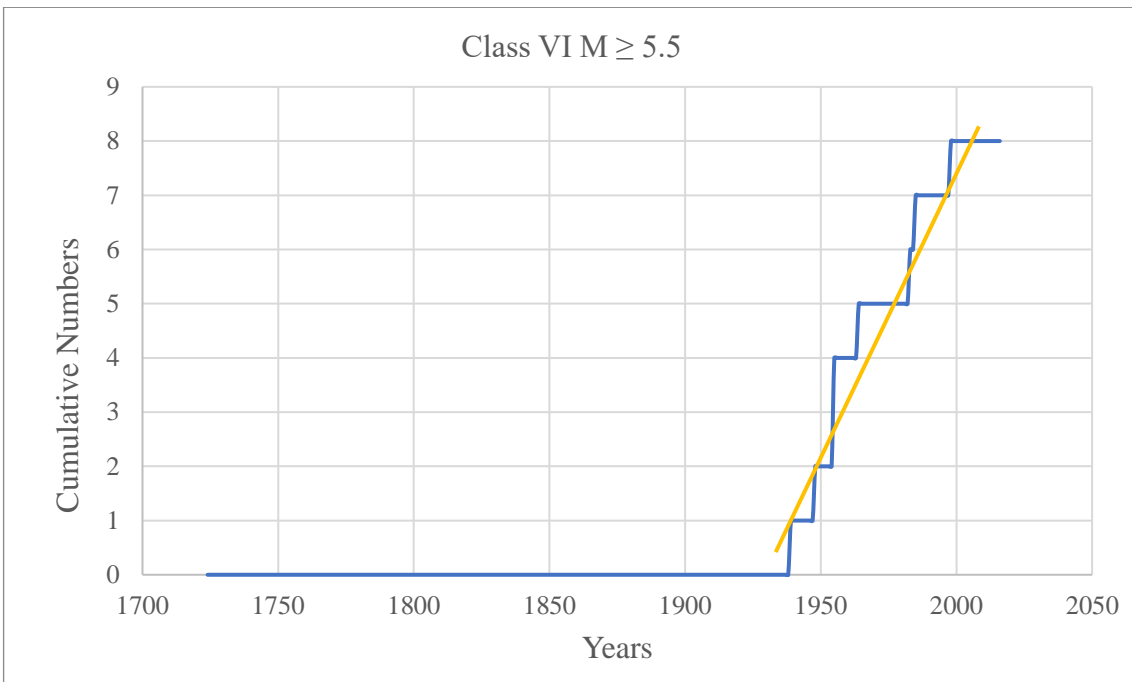


Figure 14 - Identification of the completeness period for class of magnitude $\geq 5,5$

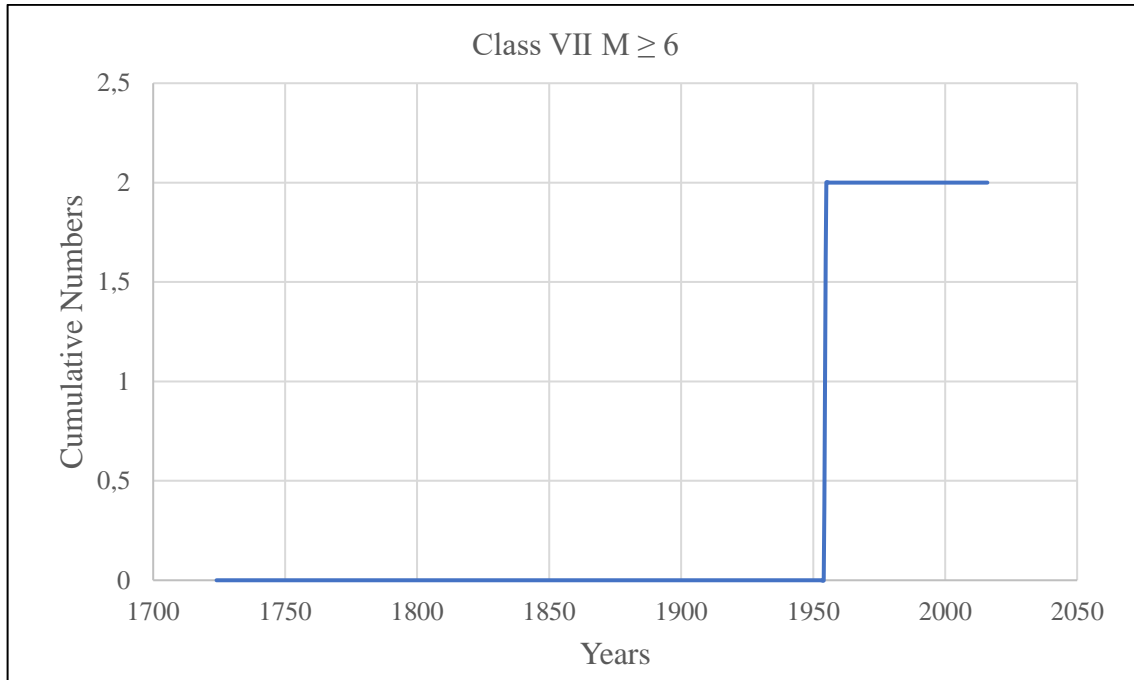


Figure 15 - Identification of the completeness period for class of magnitude $\geq 6,0$

Magnitude Classes Mw	Completeness Periods
3,0	1980
3,5	1980
4,0	1960
4,5	1910
5,0	1888
5,5	1870
6,0	1850

Table 2 - Completeness Periods

Brazil is not an active seismic zone, consequently the number of events in the history of the country with magnitude $M_w \geq 4,5$ is low. Based on that, it is possible to notice that the classes of magnitude 5,5 and 6,0 cannot be approximated by a straight line. The completeness periods for these two classes were defined after a thoroughly revision of the articles done by Dourado (2013) and Assumpção et al. (2018), and based on the catalogue data of this study. The completeness periods from 3,0 up to 4,5 were taken from the graphics above and the completeness periods from 5,0 , 5,5 and 6,0 were defined based on the catalogue data for this study and previous studies.

3.2 SEISMIC SOURCE ZONES AND PARAMETERS

The earthquake catalogue is unlikely to be a sufficient basis for defining the spatial distribution of future earthquakes. The Cornell method (1968), in its original formulation, the earthquakes sources were represented only as an areal zone or line zones (faults) that, based on geological, seismological and historical evidence, could be regarded as homogeneous; this means that each small portion of a zone can generate an earthquake of given magnitude with the same probability as any other portion of the same zone. The earthquakes are considered to “be equally likely at any location in the source zone and it is also assumed that recurrence rates, focal depth distribution, style-of-faulting and the maximum seismogenic potential are all constant across the seismic source zone.” (Asumpção et al. , 2018).

Considering from now on only the Southeastern region of Brazil, the region of this case study, the working catalog was filtered to consider only Rio de Janeiro, Minas Gerais, São Paulo and Espírito Santo states, in which there are 800 events with magnitude level from 2,7 up to 6,2, showed in Figure 16. The city of Arraial do Cabo ($22^{\circ} 57' 57''$ S, $42^{\circ} 1' 40''$ W), located in the Rio de Janeiro state, is the site for the evaluation of the seismic hazard. This choice is justified by the fact that Arraial do Cabo is an approximately baricentric position in defined seismic zones and is the easternmost city of the southeastern region, with important geographical location in relation to offshore activities.

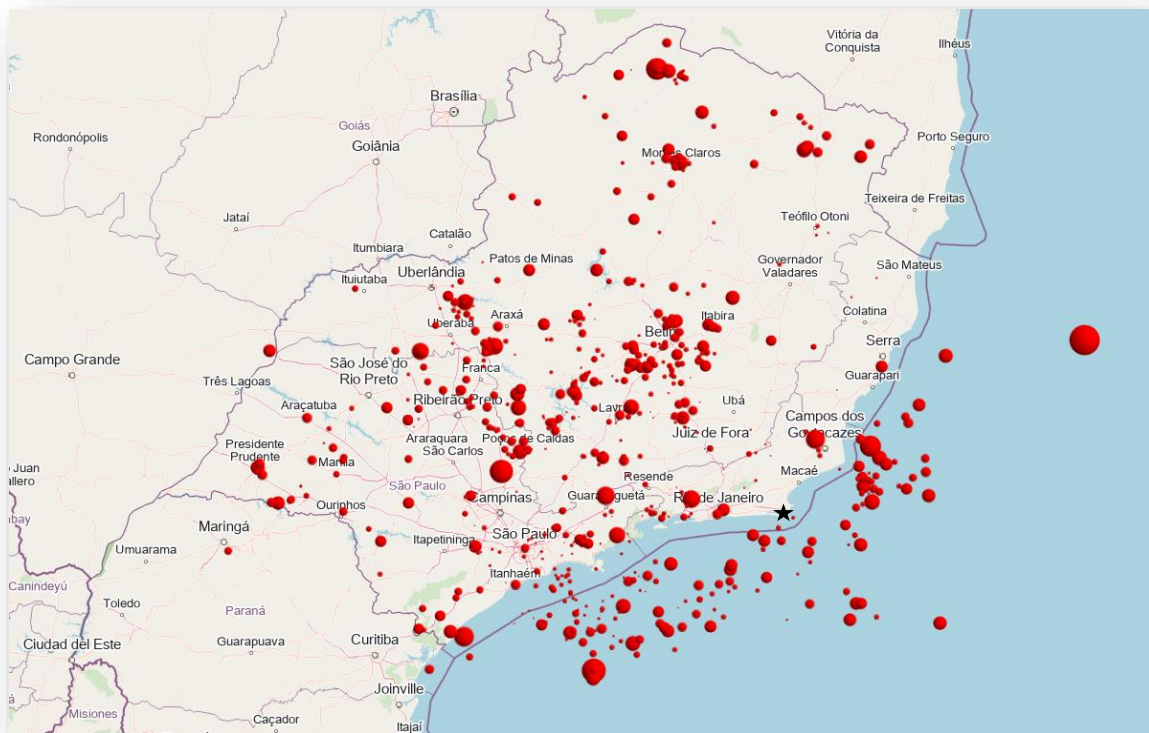


Figure 16 - Earthquakes events of southeastern Brazil from working catalog. Site of Arraial do Cabo city marked on the map with a star.

This region, showed in figure 16 with the events of the working catalogue, was separated in three models of seismogenic zones for this study. Model 1) with unique seismic zone including Rio de Janeiro, Minas Gerais, São Paulo and Espírito Santo states, and continental shelf; Model 2) with two zones, one seismic zone including the states of Rio de Janeiro, Minas Gerais, São Paulo and Espírito Santo, and another one including the continental shelf; Model 3) with three zones, one seismic zone including Minas Gerais and part of Sao Paulo, one seismic zone considering the coastal part, which includes Espírito Santo, Rio de Janeiro and São Paulo , and one seismic zone for the continental shelf. The illustration of these seismogenic zones models for this study will be shown in the following section.

Brazil does not have official seismogenic zones, the published papers about seismic hazard on the country have created zone models considering the most important economic states, an example is the work done by Hampshire and Lima (2008) describing the Brazilian standard for seismic design on the southeast region. This same idea is reproduced in this

study, considering the most important economic and populated region of the country. A geologic basis to define the seismic zones models was not applied because is conservatively considered that the seismicity of the southeastern is concentrated and is uniformly distributed in this area bounded by the red dots in figure 16. The goal is starting with a great seismogenic zone model and then subdividing it in smaller zones analyzing how it affect the R-CRISIS program results of probabilistic seismic hazard analysis. In other words, the idea is checking in how the size of seismic zone models affects the R-CRISIS results.

After defining the vertices of the seismogenic zone cases, the next step is describing the relative frequency of occurrence of stronger events with respect to low to moderate events. Each seismic source zone can be described by a single frequency-magnitude relationship $v = v(M)$, where v is the annual occurrence rate of earthquakes with magnitude $\geq M$ and, hence, by a single magnitude distribution $F_M(m)$ typically truncated at lower (M_{min}) and at an upper (M_{max}) magnitude bound. The seismic activity of the source zone is quantified through Gutenberg and Richter, GR (1956) relationship:

$$\log v = a - (b \times M) \quad (2)$$

Where, a-value is the logarithm of the number of events with $M \geq 0$ and consequently an indicator of the seismic activity; and b-value is a positive number which describes the slope of the generally linear relationship between $\log v$ and M .

Setting:

$$\beta = b \times \ln 10 \quad (3)$$

$$\alpha = a \times \ln 10 \quad (4)$$

Then, the annual occurrence rate of earthquakes is computed as:

$$v(Mmin) = e^{\alpha - \beta \times Mmin} \quad (5)$$

The procedure to find these parameters for the GR relationship for each seismic source zone has the following steps:

- 1) The completeness analysis of the working catalog gave K completeness classes with their completeness period range, T_{ck} , related to year 2016:

Magnitude	Completeness Period	Period Range (T_c)	2016
3,0	1980	36	
3,5	1980	36	
4,0	1960	56	
4,5	1910	106	
5,0	1888	128	
5,5	1870	146	
6,0	1850	166	

Table 3 - completeness classes with their completeness period range, T_{ck} , according to the reference year 2016.

- 2) Selection of a lower threshold m_o :

The minimum magnitude m_o is chosen considering the engineering significance of an earthquake occurrence. For this case study the lower threshold is $m_o = 4,0$.

- 3) Subdivision of all $M \geq m_o$ in intervals of equal ΔM .
- 4) For each ΔM_i , take the value of M_i as representative.
- 5) Computation of the number of earthquake events n_{ik} , within completeness class K, with magnitude belonging to interval ΔM_i ;
- 6) Computation of cumulative rates of occurrences for M_i rates of events with magnitude $M \geq M_i$:

$$v = \sum \frac{n_{ik}}{T_{ck}} \quad (6)$$

- 7) Plot of the M_i values, of each ΔM_i , with corresponding cumulative rates of occurrences.

The temporal occurrence of earthquakes is commonly described by a Poisson model. This model provides a simple framework for evaluating probabilities of events that follow Poisson process, it means that yields values of a random variable describing the number of occurrences of a particular event during a given time interval.

Under the assumption that a lower and an upper threshold exist, it means that if in the seismogenic zone there are no faults capable to produce an earthquake with magnitude $M > m_1$, the probability distribution of magnitude can be easily shown to be:

$$F_M(m) = P(M \leq m | m_0 \leq M \leq m_1) = \frac{1 - e^{-\beta(m-M_0)}}{1 - e^{-\beta(M_1-M_0)}} \quad (7)$$

Considering that $M \geq m_0$ and $M \leq m_1$.

Therefore, the classical Gutenberg – Richter relationship for the earthquake occurrence rates is the basis for the standard description of a truncated exponential magnitude distribution and a Poissonian recurrence process, that is, independence between magnitude and interevent times. This approximation is satisfactory also when low seismicity areas are considered. This Poisson model provides a simple framework for evaluating probabilities of events that follow this Poisson process.

The basic assumption in Cornell (1968) is that earthquake occurrences follow this Poisson process in time. The properties of Poisson process are: the number of occurrences in one time interval are independent of the number that occur in any other time interval; the probability of occurrence during a very short time is proportional to the length of the time interval and the probability of more than one occurrence during a very short time interval is negligible. The important implications about Poisson process are that there is no memory of the past earthquakes and the chance of an earthquake occurring in a given year does not depend on how long it has been since the last event, and the temporal occurrence distribution is independent of the magnitude distribution.

Thus, the number of events of interest, N_t , in a time interval of t years is Poisson distributed as shown in equation 8.

$$P(N_t = n) = \frac{(vt)^n e^{-vt}}{n!} \quad n = 0,1,2 \dots \quad (8)$$

Consider now that earthquake events are Poisson arrivals with average rate v and that each event has a probability p of being an event that generates a ground motion exceeding the limit y at a site of interest independently of the others. These events are Poisson arrivals with average vp (“random selection” property). Hence, the probability that the ground motion at a site exceeds n times y in t is:

$$P(N_t = n) = \frac{(vpt)^n e^{-vpt}}{n!} \quad n = 0,1,2 \dots \quad (9)$$

Based in all these hypotheses and assuming a statistical independence among the different earthquake sources that contribute to the hazard, the number of events per year, λ , exceeding a specific shaking level y at a site, called annual frequency of exceedance, inverse of return period, can be written as:

$$\lambda (Y \geq y) = \sum_{i=1}^I v_i p \quad (10)$$

The following sections will show the computations to find the GR relationship and then the annual occurrence rate of earthquake for each the three cases of seismic source zones. The annual occurrence of events, the vertices of the seismic zone and the defined values of maximum and minimum magnitudes are the input for the seismic hazard analysis in the R-CRISIS program.

3.2.1 SEISMIC SOURCE ZONE MODEL 1

This first seismic source zone model regards the entire Southeast region including the continental shelf. The states of Brazil belonging to the Southeast are Rio de Janeiro, São Paulo, Belo Horizonte and Espírito Santo. The vertices of this seismic source zone is shown in the figure below and it will be called zone (1a). The site Arraial do Cabo is represented with a star point.

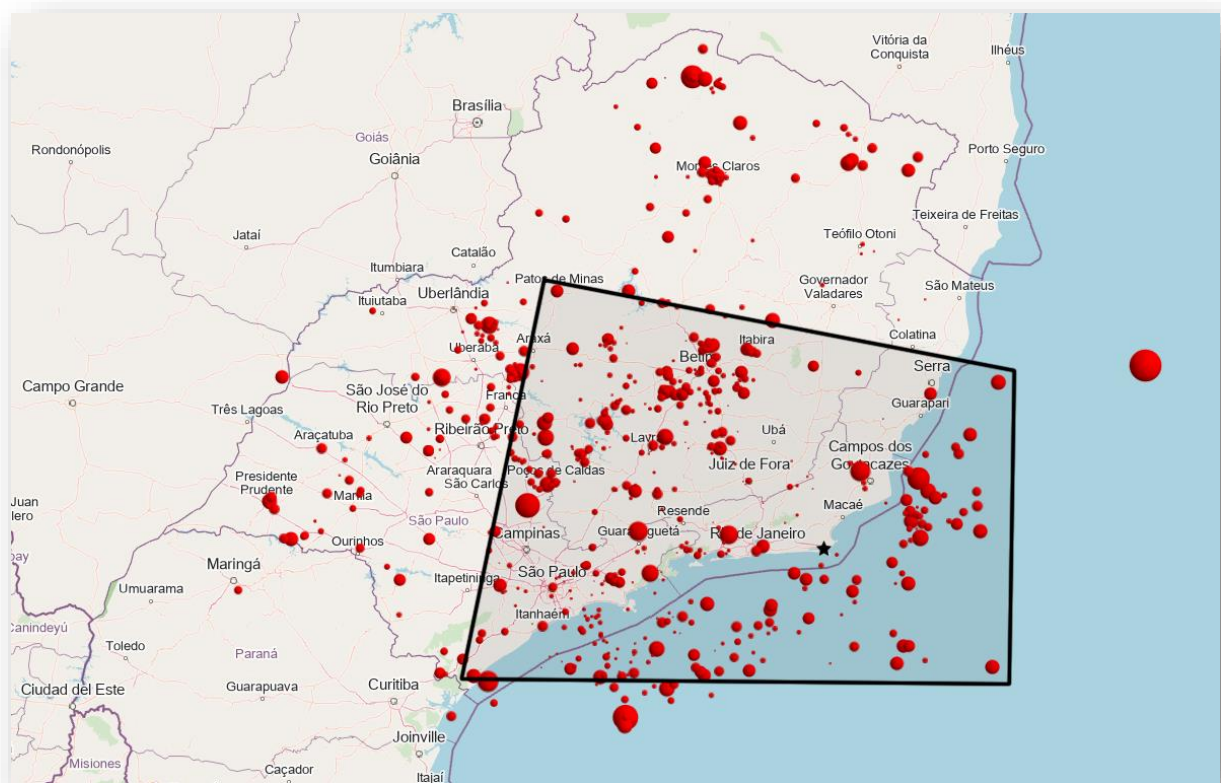


Figure 17 - Seismic source zone 1a

SEISMIC ZONE 1a		
Vertex	Latitude	Longitude
1	-25,01	-47,94
2	-18,60	-46,55
3	-20,12	-39,20
4	-24,86	-39,30
Arraial do Cabo	-22,93	-42,04

Table 4 - Seismic zone (1a) and site coordinates

The lower threshold m_0 is 4,0 , however the procedure of finding the GR relationship will consider magnitudes greater or equal to 3,0 in an attempt to be as accurate as possible to find the straight line coefficients. The lower threshold will be used to compute $v(M)$, the annual occurrence rate of earthquakes, and as input for R-CRISIS analysis.

All the magnitudes greater or equal do 3,0 were divided in equal intervals of $\Delta M = 0,125$ and for each ΔM_i was taken the central value of M_i as representative. The number of events belonging to interval of magnitude ΔM_i is n_{ik} and the cumulative rates of occurrences, v_i , with magnitude $M \geq M_i$, for each M_i is found as shown in equation (6). Table 5 below shows the values found of cumulative rates of occurrences and $\log_{10} v_i$ for this first seismic source zone.

$M_i \pm \Delta M$	ΔM_i	$v_i = \sum (n_{ik} / T_{ck})$	$\log v_i$
$3,0 \pm 0,125$	2.875-3.125	17,423	1,241
$3,25 \pm 0,125$	3.125-3.375	11,821	1,073
$3,5 \pm 0,125$	3.375-3.625	7,215	0,858
$3,75 \pm 0,125$	3.625-3.875	4,043	0,607
$4,0 \pm 0,125$	3.875-4.125	2,169	0,336
$4,25 \pm 0,125$	4.125-4.375	0,929	-0,032
$4,5 \pm 0,125$	4.375-4.625	0,293	-0,534
$4,75 \pm 0,125$	4.625-4.875	0,109	-0,964
$5,0 \pm 0,125$	4.875-5.125	0,092	-1,035
$5,25 \pm 0,125$	5.125-5.375	0,065	-1,187
$5,5 \pm 0,125$	5.375-5.625	0,028	-1,556
$5,75 \pm 0,125$	5.625-5.875	0,000	-
$6,0 \pm 0,125$	5.875-6.125	0,000	-

Table 5 - Cumulative rates of occurrences and $\log_{10} v_i$ for seismic source zone (1a)

The plot of M_i values for each magnitude interval with corresponding logarithm of the cumulative rates of occurrence is shown in the figure 18. The annual frequency of earthquake or Gutenberg-Richter relationship is quantified by the linearization of the plot results, the straight-line coefficients are the parameters a and b shown in the equation (2).

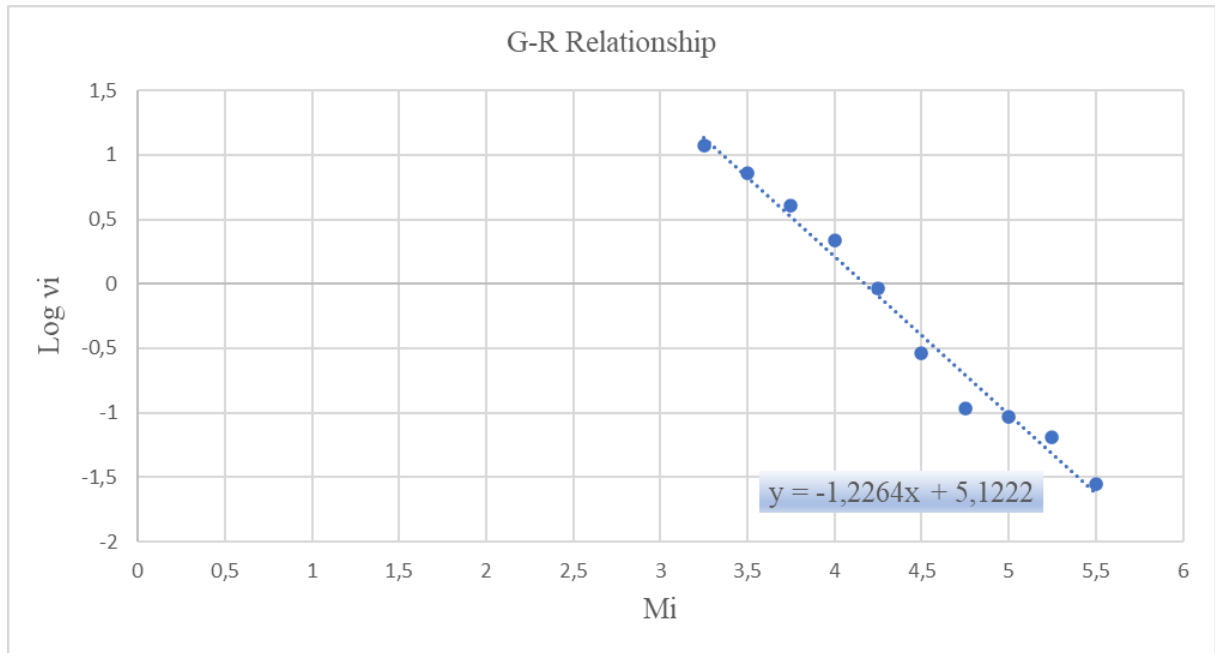


Figure 18 - GR relationship to seismic zone (1a)

On the table 6 is shown the final computation for the annual occurrence rate of earthquakes with magnitude $\geq 4,0$.

log v = -1.226M + 5.122	
a	5,122
b	1,226
$\beta = b \cdot \ln 10$	2,824
$\alpha = a \cdot \ln 10$	11,794
Mmin	4,0
$v_0(4,0) = e^{\alpha - \beta \times Mmin}$	1,647

Table 6 - GR relationship parameters and final computation of annual occurrence rate of earthquakes.

3.2.2 SEISMIC SOURCE ZONE MODEL 2

The second model includes two zones, a continental portion and the continental shelf. One seismic source zone covering the states of Rio de Janeiro, Minas Gerais, São Paulo and Espírito Santo, shown in Figure 19 and called seismic zone (2a), and another one containing the continental shelf as in Figure 20 and called seismic zone (2b).

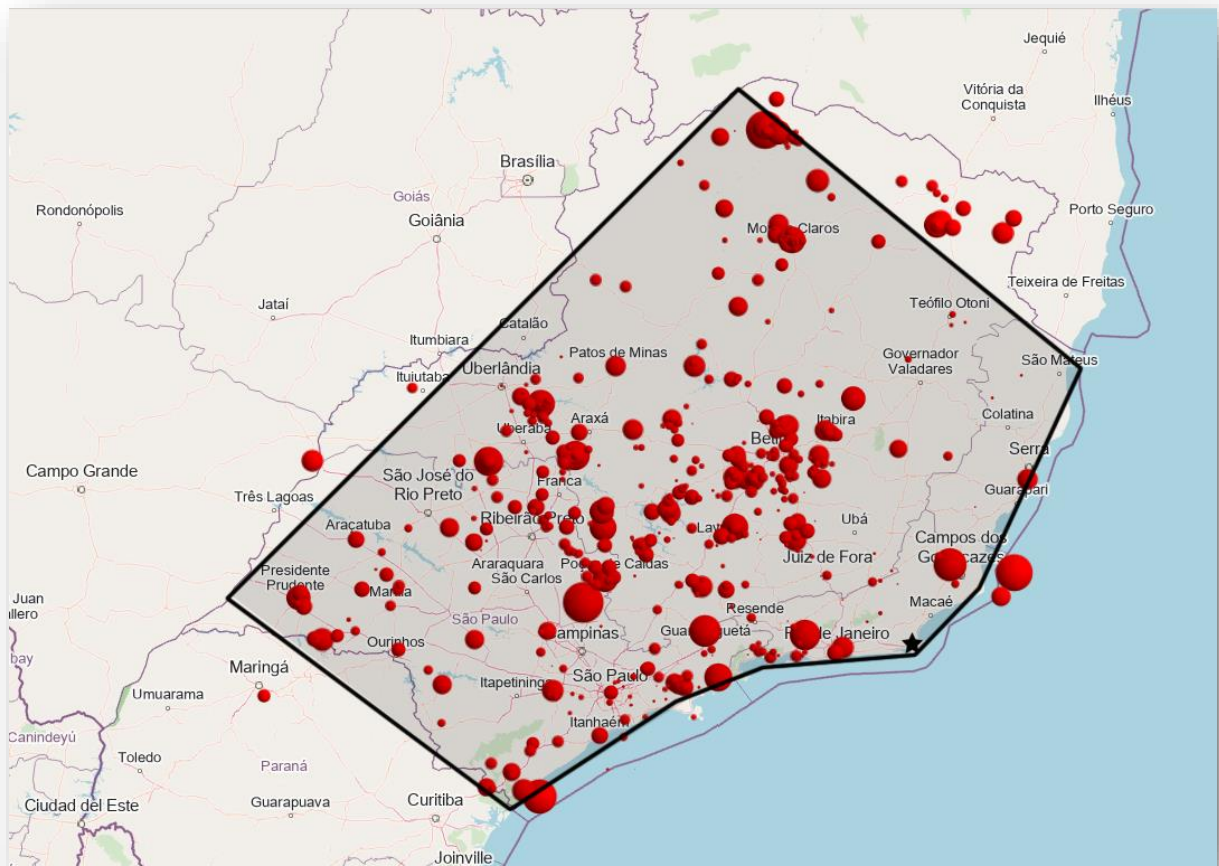


Figure 19 - Seismic source zone model 2: continental portion , seismic zone (2a)

SEISMIC ZONE (2a) : continent part		
Vertex	Latitude	Longitude
1	-14,37	-44,68
2	-18,63	-39,52
3	-21,96	-40,99
4	-22,93	-42,04
5	-23,1	-44,24
6	-25,28	-48,26
7	-22,11	-52,43
Arraial do Cabo	-22,93	-42,04

Table 7 - Seismic zone and site coordinates: continental portion

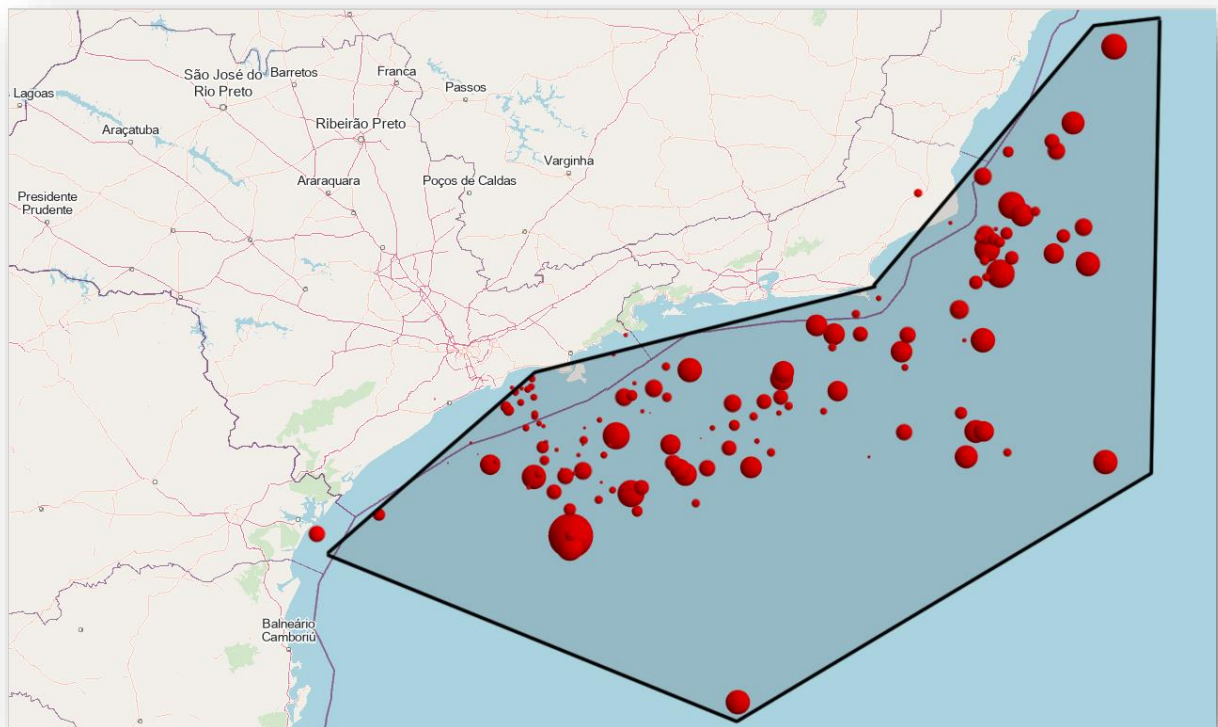


Figure 20 - Seismic source zone model 2: continental shelf, zone (2b)

SEISMIC ZONE (2b) : continental shelf		
Vertex	Latitude	Longitude
1	-19,93	-39,44
2	-19,9	-38,8
3	-24,94	-38,76
4	-27,8	-43,5
5	-25,93	-48,2
6	-23,85	-45,88
7	-22,93	-42,04
Arraial do Cabo	-22,93	-42,04

Table 8 - Seismic zone and site coordinates: continental shelf

The same procedure as explained before with the first model of seismic source is done here again for each seismic source zone (continental portion and continental shelf) and the final value for the annual occurrence rate of earthquakes with magnitude $\geq 4,0$.

The results of each computation step are plotted for the GR relationship and the final goal, the annual occurrence rate of events, will be shown by the following graphics and table below showing the results for the continental portion and for the continental shelf.

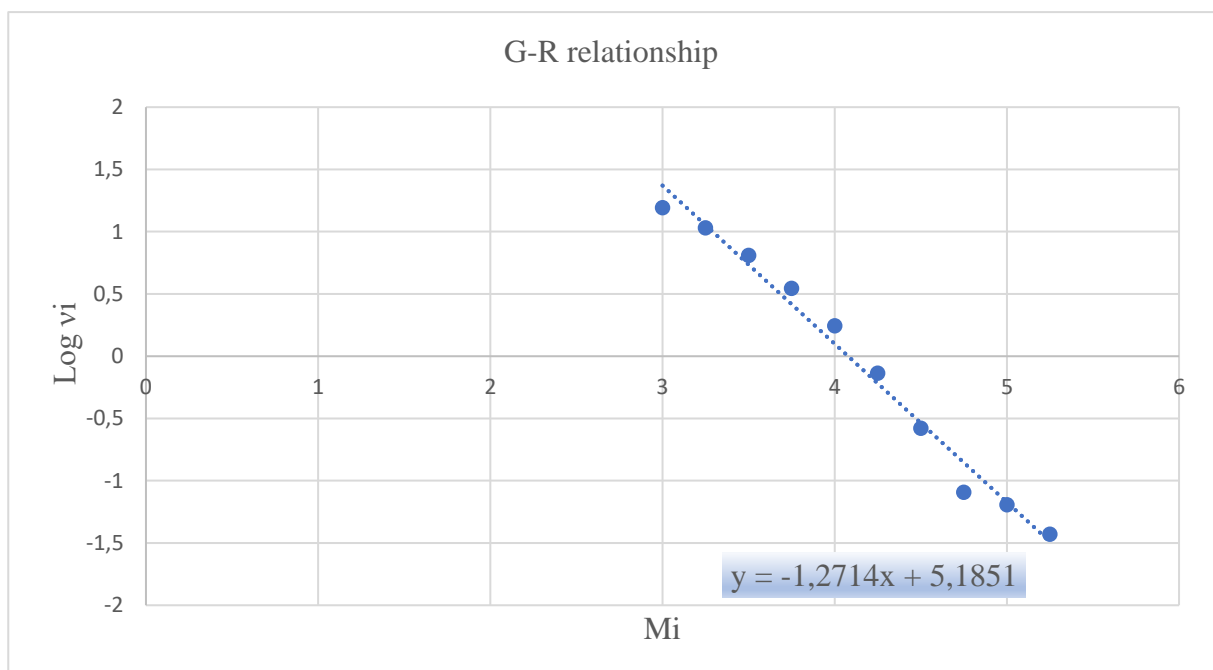


Figure 21 - GR relationship of seismic source zone model 2- (2a) : continental portion

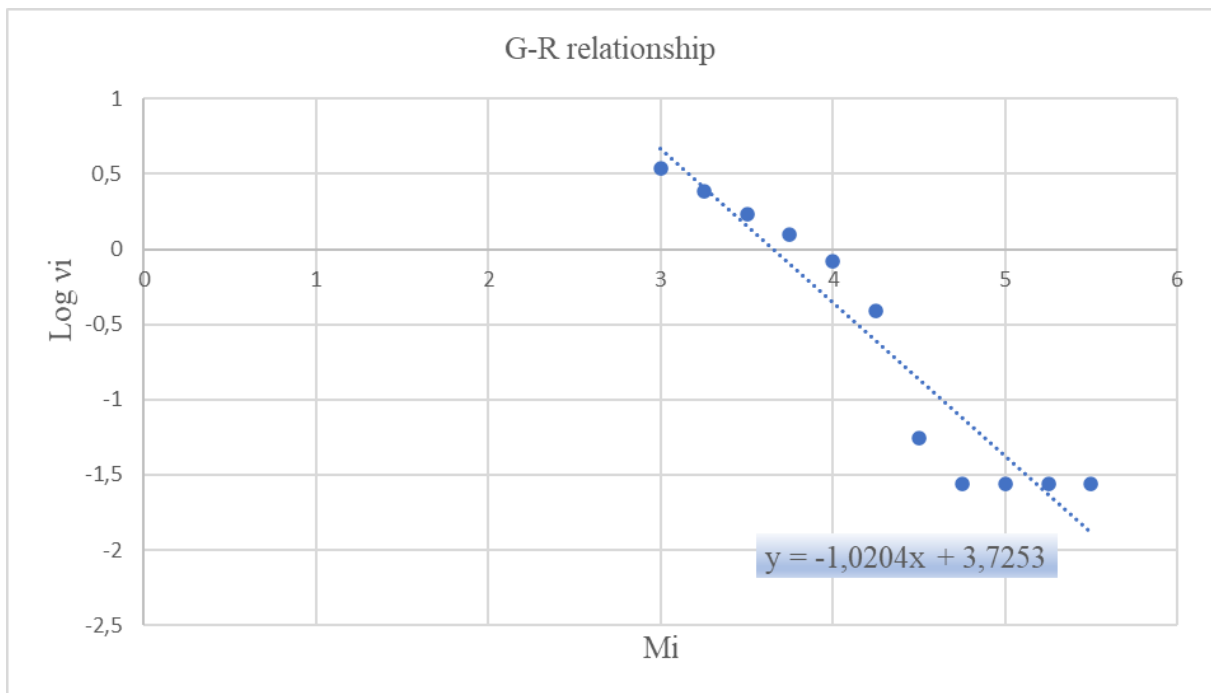


Figure 22 - GR relationship of seismic source zone model 2 – (2b): continental shelf

	Seismic zone (2a)	Seismic zone (2b)
	$\log v = -1.271M + 5.185$	$\log v = -1.024M + 3.725$
a	5,185	3,725
b	1,271	1,024
$\beta = b \cdot \ln 10$	2,928	2,358
$\alpha = a \cdot \ln 10$	11,939	8,578
Mmin	4,0	4
$v_0(4,0) = e^{\alpha - \beta \times Mmin}$	1,257	0,426

Table 9 - GR relationship parameters and final computation of annual occurrence rate of earthquakes

3.2.3 SEISMIC SOURCE ZONE MODEL 3

The third model of seismic zone for the analysis includes one seismic source zone for Minas Gerais state and part of São Paulo state, called by zone (3a), another one for the coastal part, which includes Espírito Santo, Rio de Janeiro and São Paulo states, called by zone (3b), and one last source zone for the continental shelf called by zone (3c), the same considered in analysis of model 2. The representation of this third case of seismic source zones for the continental portion with two seismic zones for analysis is shown in the figure 23 below and the vertices coordinates on the table 10.

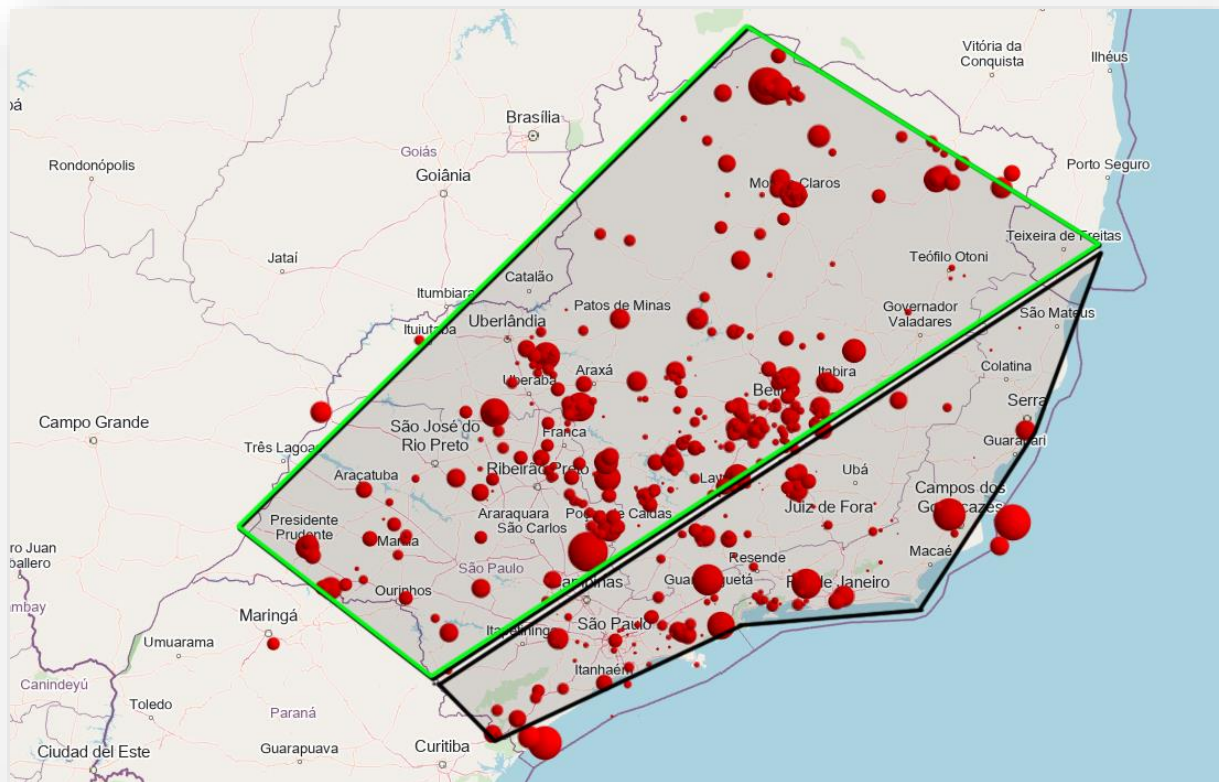


Figure 23 - Representation of seismic zones of model 3 - the continental portion which are zones (3a) and (3b), green and black areas, respectively.

SEISMIC ZONES				
	Seismic zone (3a) - Green Area		Seismic zone (3b) - Black Area	
Vertex	Latitude	Longitude	Latitude	Longitude
1	-20,89	-45,55	-17,77	-39,22
2	-17,68	-39,19	-20,38	-40,20
3	-23,97	-49,52	-22,93	-42,04
4	-21,70	-32,81	-23,41	-44,00
5			-25,05	-48,49
6			-24,12	-49,39
Arraial do Cabo	-22,93	-42,04	-22,93	-42,04

Table 10 - Seismic zones and site coordinates of the continental portion

The computation of cumulative rates of occurrences and the logarithm of these values for the two seismic source zones were done and the plot of M_i values for each ΔM_i with corresponding logarithm of the cumulative rates of occurrence is shown in figures 24 and 25.

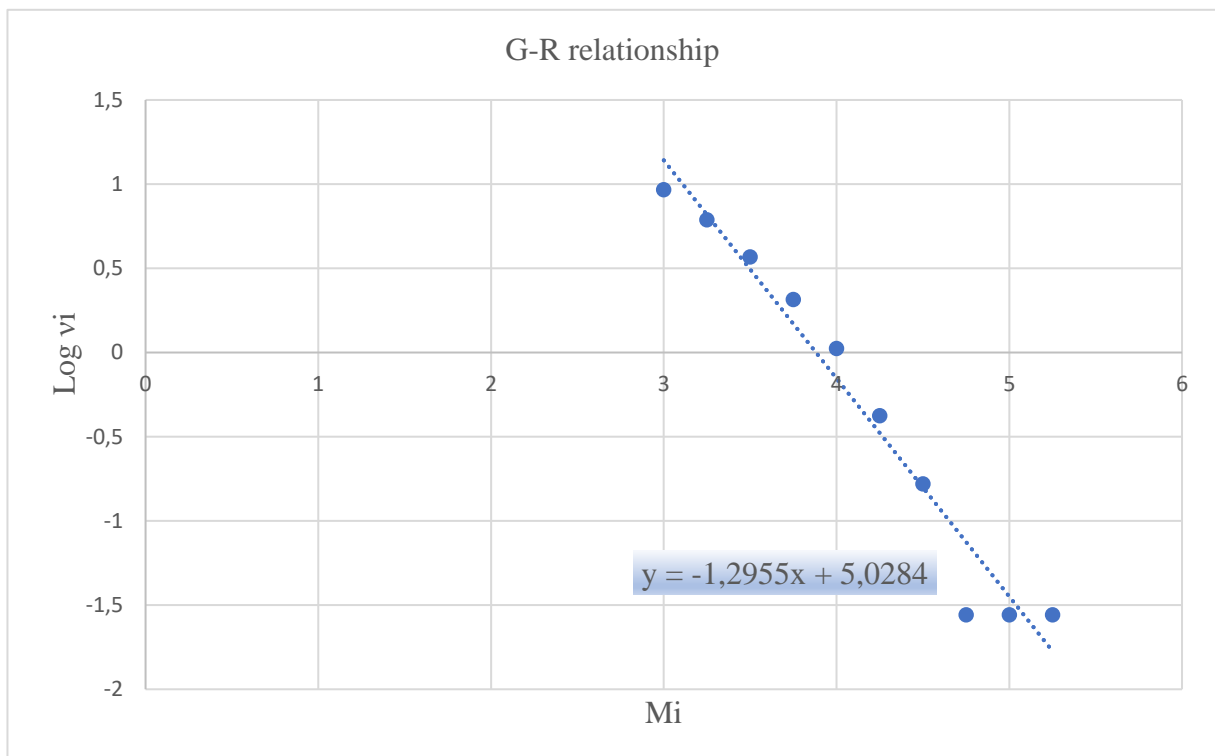


Figure 24 - GR relationship of seismic source zones model 3 – (3a) : including Minas Gerais and part of São Paulo

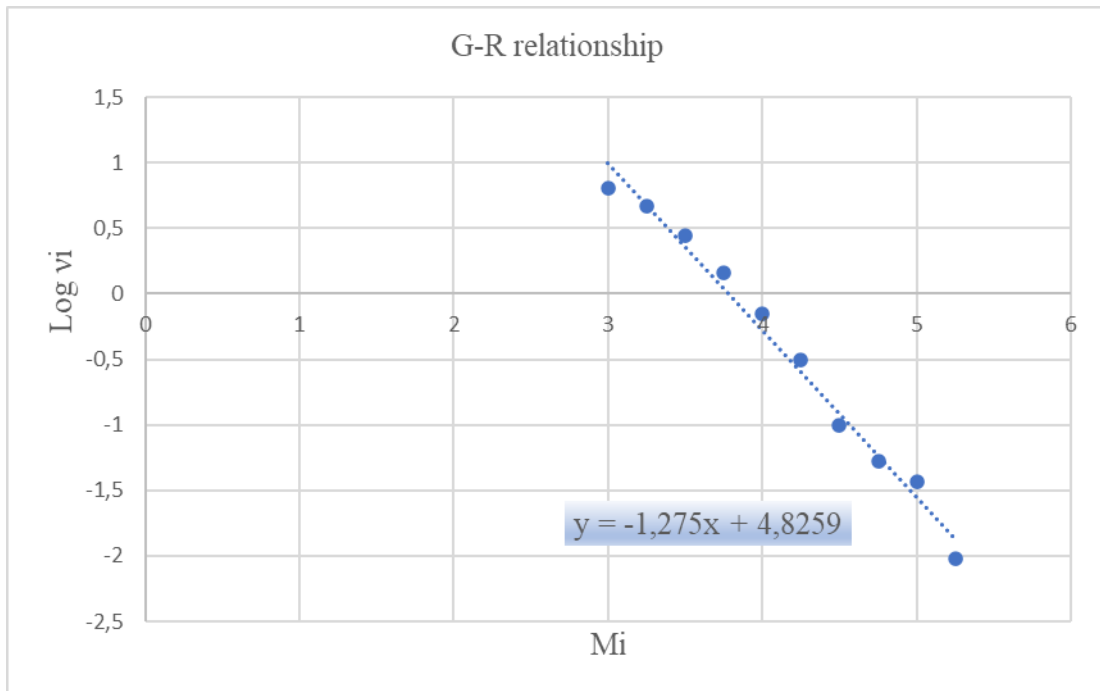


Figure 25 - GR relationship of seismic source zones model 3- (3b) : including part of São Paulo, Rio de Janeiro and Espírito Santo

The straight-line coefficients from the Gutenberg-Richter relationship are the parameters a and b for the annual frequency of earthquakes events formula computed with the minimum magnitude 4,0. On table 11 below is possible to check the final values found for each seismic source zone from continental portion of model 3.

	Seismic zone (3a)	Seismic zone (3b)
	$\log v = -1.296M + 5.028$	$\log v = -1.275M + 4.826$
a	5,028	4,826
b	1,296	1,275
$\beta = b \cdot \ln 10$	2,983	2,936
$\alpha = a \cdot \ln 10$	11,578	11,112
M_{min}	4,0	4,0
$v_0(4,0) = e^{\alpha - \beta \times M_{min}}$	0,702	0,532

Table 11 - GR relationship parameters and final computation of annual occurrence rate of earthquakes for (3a) and (3b) areas of the seismic zones from the continental portion

The model of seismic source zone analyzed in this chapter considers three zones, which two of them from the continental portion have already computed their parameters for the annual occurrence rate of events. The third zone considered in this case is the continental shelf, already computed in the previous chapter of this work study, called now by seismic zone (3c). The final parameters for the continental shelf are shown again on table 12 below.

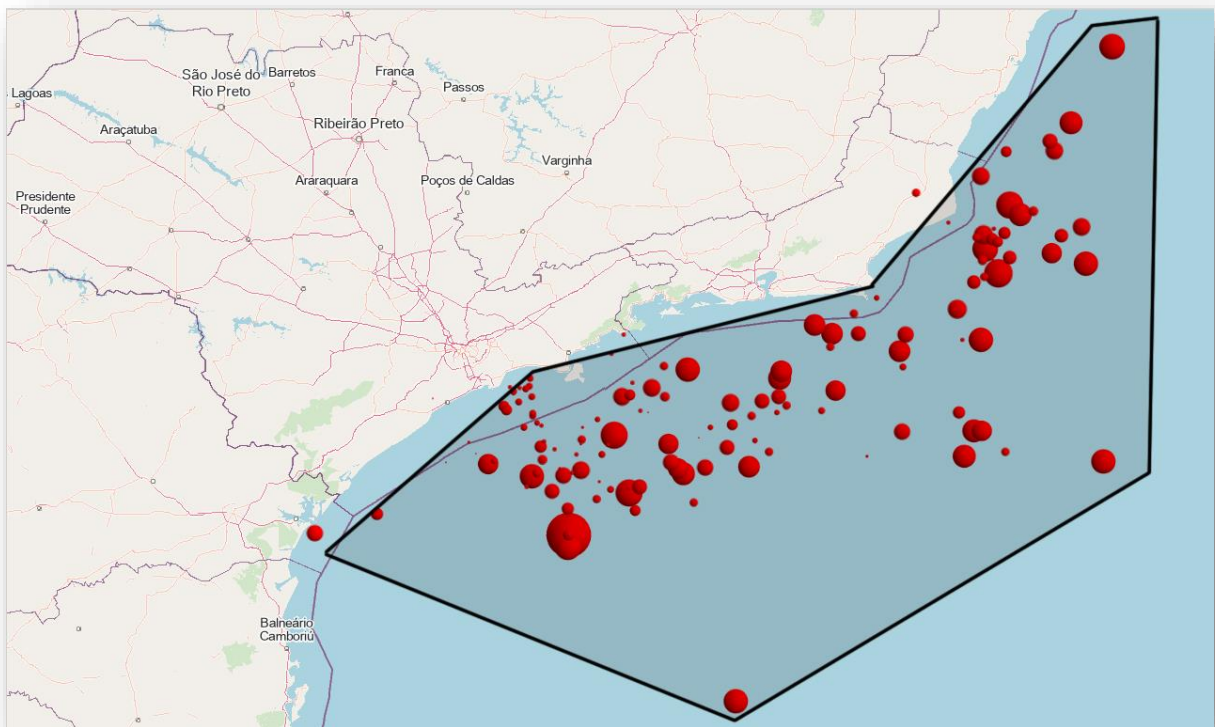


Figure 26 - Seismic source zone case model 3 – (3c) : continental shelf

$\log v = -1.024M + 3.725$	
a	3,725
b	1,024
$\beta = b \cdot \ln 10$	2,358
$\alpha = a \cdot \ln 10$	8,578
Mmin	4,0
$v0(4,0) = e^{\alpha - \beta \times Mmin}$	0,426

Table 12 - GR relationship parameters and final computation of annual occurrence rate of earthquakes for continental shelf

3.2.4 ANALYSIS OF G-R RELATIONSHIP FOR THE SEISMIC ZONE MODELS

The Gutenberg–Richter relation for earthquake magnitudes is the most famous empirical law in seismology. It expresses the relationship between the earthquake magnitude and number of earthquakes per year of magnitude. The parameters a and b of this relation are important to describe the seismic zone. The a -value represents the total seismicity rate of the region and the b -value is crucial for evaluation of the earthquake occurrence probability, it quantifies the ratio of large-to-small earthquakes and is commonly close to 1,0 in seismically active regions. If $b < 1,0$, then the frequency of larger earthquakes is higher than the small and moderate ones, so it is defined as a high seismic danger area.

The analysis done to find the GR relation for each seismic source zone in each defined model is summarized in the table below.

	Model 1	Model 2		Model 3		
	SZ (1a)	SZ (2a)	SZ (2b)	SZ (3a)	SZ (3b)	SZ (3c)
G-R relation	$\log v = -1,226M + 5,122$	$\log v = -1,271M + 5,185$	$\log v = -1,024M + 3,725$	$\log v = -1,296M + 5,028$	$\log v = -1,275M + 4,826$	$\log v = -1,226M + 5,122$
a-value	5,122	5,185	3,725	5,028	4,826	3,725
b-value	1,226	1,271	1,024	1,296	1,275	1,024
$\beta = b \cdot \ln 10$	2,824	2,928	2,358	2,983	2,936	2,358
$\alpha = a \cdot \ln 10$	11,974	11,939	8,578	11,578	11,112	8,578
$v_0 = e^{\alpha - \beta \times M_{min}}$	1,647	1,257	0,426	0,702	0,532	0,426

Table 13 - Final parameters for each seismic zone

With reason to these results, it is notable that b -value is greater than 1,0 but not higher than 1.5. This means that the frequency of smaller earthquakes is more usual than larger earthquakes, this describes the example of stable continents seismicity. The graphics with $\log v$ and M show that the linearization of each plot results has a straight line with a more accentuated slope and not a more horizontal straight line as commonly in very active seismic areas.

Finally, with all the parameters defined for each case of seismic source zones the next step for the R-CRISIS program input is the description of the ground motion attenuation, the computation of $p = P (Y \geq y)$ from equation (10), generally performed using empirical ground motion equation models. The next chapter will explain the context behind the GMPEs and the selection of them.

3.3 GROUND MOTION PREDICTION EQUATIONS

The relationships that link a particular ground motion parameter with the quantities that control it are called ground motion prediction equations (GMPEs). Predictive relationships usually express ground motion parameters as functions of magnitude (M), source-to-site distance (R), site classification and other variables in some cases.

The source-to-site distance can be interpreted in different ways. The hypocentral (R_{yp}) and epicentral (R_{epi}) distances are the easiest to be calculated and represent the distance from the site to the hypocenter and its projection on the surface (epicenter). However, in earthquakes for which the length of fault rupture is large, the fault distance or rupture distance (R_{rup}) is more important and can be quite different from the hypocenter. Another commonly used distance metric is the Joyner and Boore distance (R_{JB}) that represents the closest distance from the surface projection of the fault.

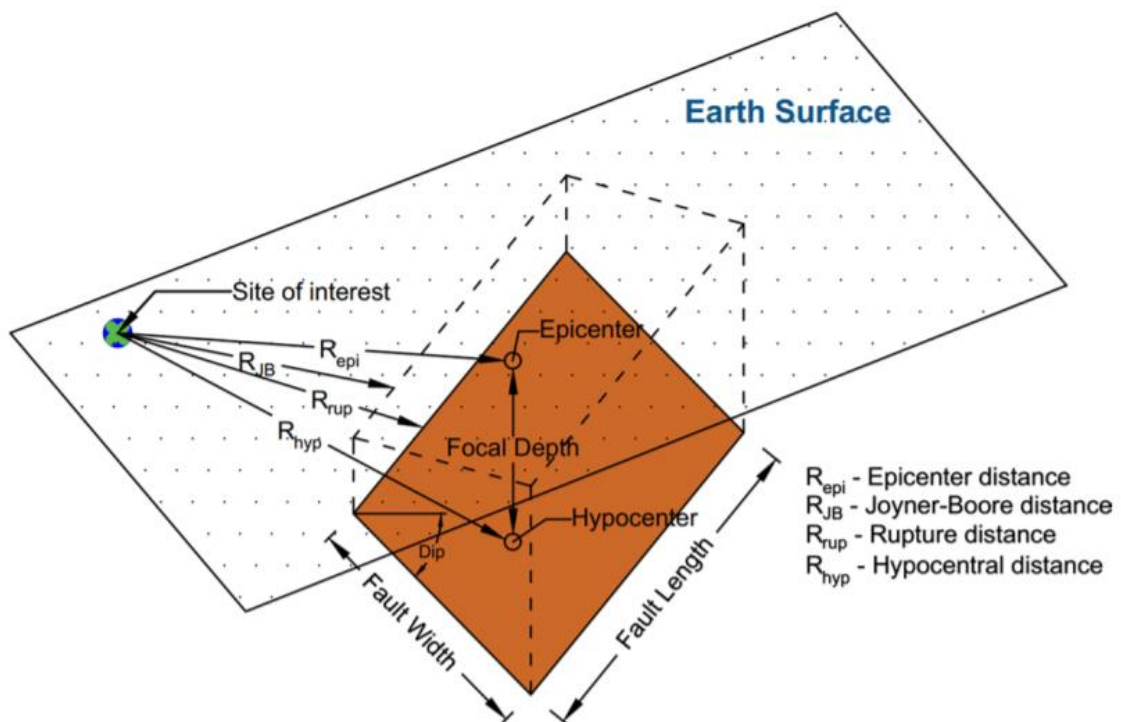


Figure 27 - Definition of the distance metrics usually used in the GMPEs. Taken from Ilya Sianko et al., 2019, *A practical probabilistic earthquake hazard analysis tool: case study Marmara region*.

The ground motion relationships are developed by regression analyses of recorded strong motion databases and the functional form of the predictive relationship is usually selected to reflect the mechanics of the ground motion process as closely as possible. The regression is performed on the logarithm of y , ground motion parameter of interest, because peak values of strong motion are approximately lognormally distributed.

$$y = f(\underline{x}) \quad (11)$$

Where y is the ground motion parameter of interest (peak ground acceleration; peak velocity; spectral ordinates) and \underline{x} is independent predictive parameters (magnitude; distance; epicentral intensity ; site class).

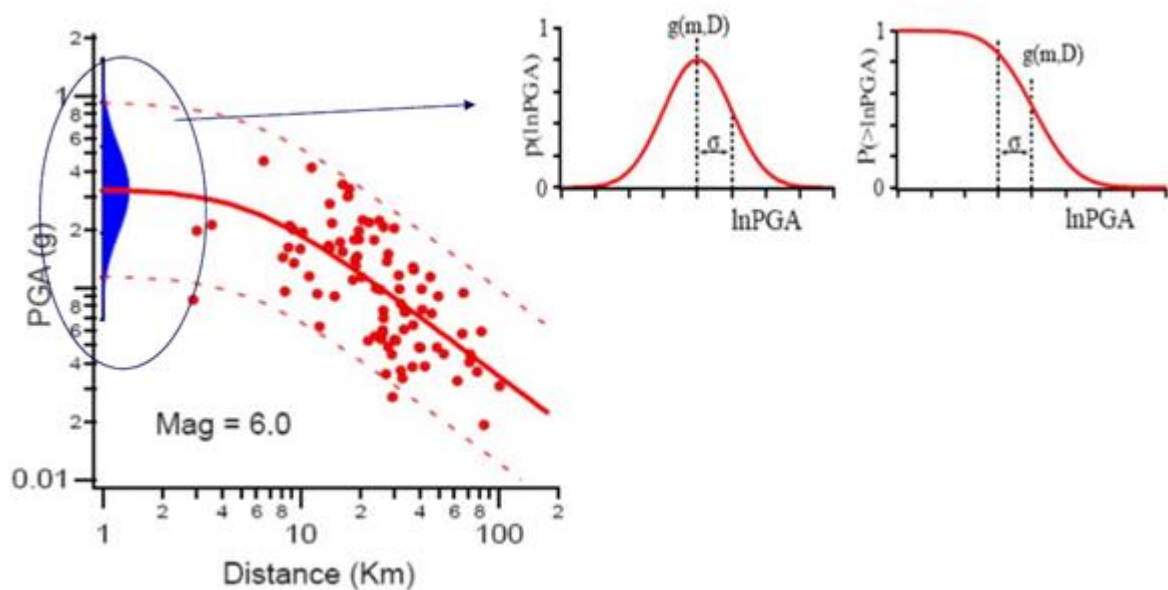


Figure 28 - Ground motion parameters lognormally distributed.
From Boore, Joyner and Fumal, 1997.

A GMPE is typically of the form:

$$\log y = const + f(M) + f(r, M) + f(source) + f(site) \pm \varepsilon \quad (12)$$

Where, M is the magnitude, r is a measure of the source-to-site distance and the error ε , or logarithmic residual, is an aleatory variable with zero means and standard deviation σ , which describes the uncertainty associated to the prediction.

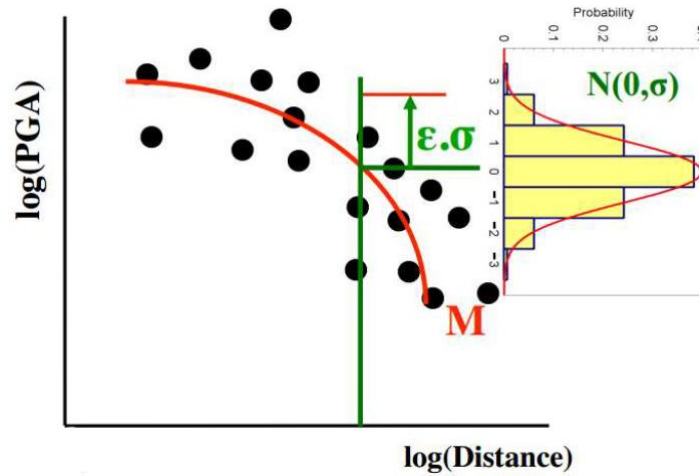


Figure 29 - GMPE error normal distribution and deviation standard. Taken from engineering seismology course slides, Politecnico di Milano, 2018.

Through the attenuation relation, the probability that a ground motion parameter Y exceeds a certain threshold y for an earthquake of given magnitude m occurring at distance r from the site. Once $f_r(r)$ is known, the probability $P[Y > y]$ for the entire seismic zone is completely defined by:

$$P(Y > y | m, r) = 1 - F_{Y|m,r}(y) = \int_{SZ} P[Y > y | R = r] f_r(r) dr \quad (13)$$

Where $F_{Y|m,r}(y)$ is the cumulative distribution function of Y , for specified m and r . With the hypothesis that homogeneous seismic zones are considered, it means that earthquakes are assumed to equally likely occur at any location of the source, then $f_r(r)$ depends on the shape of the seismic zone and the source-to-site distance. Finally, the probability of exceeding a ground motion level y at a given site can be written as:

$$P(Y > y) = \iiint P(Y > y | m, r, \varepsilon) f_M(m) f_r(r) f_\varepsilon(\varepsilon) dm dr d\varepsilon \quad (14)$$

Where $f_M(m)$, $f_r(r)$ and $f_\varepsilon(\varepsilon)$ denote the probability density functions of the magnitude, the distance and the error of attenuation equation respectively.

The “critical events” ($Y > y$) are Poissonian events with an annual occurrence rate:

$$v_y = v \cdot P[Y > y] \quad (15)$$

The probability of occurrence of k critical events in t years will be given by:

$$P[N_t = k] = \frac{(v_y \cdot t)^k}{k!} \exp(-v_y t) \quad (16)$$

Considering Y_a the maximum annual value of Y , it means the maximum acceleration in site per year, the probability distribution of Y_a is computed allowing that in one year ($t=1$) the critical events is never exceeded ($k=0$).

$$F_{Y_a}(y) = P[Y_a \leq y] = P[N_{t=1}(y) = 0] = \exp(-v_y) = \exp(-v \cdot P[Y > y]) \quad (17)$$

The Equation 17 is a double exponential function and it is expected since the probability distribution of a maximum extreme value is variable typically as a Gumbel distribution. The return period of a critical events is therefore defined as:

$$T(y) = \frac{1}{1 - F_{Y_a}(y)} \quad (18)$$

Unfortunately, there are no strong motion records available in Brazil to develop a ground motion model constrained with local data, or to calibrate foreign models with local data. For this reason, different GMPEs formulated for subduction and crust in other parts of the world are analyzed to select those that better fit with the tectonic environment in Brazil.

The ground motion prediction equations are divided in two main families, those models that are used for active seismic continent regions (ASCR) and those for stable continent regions (SCR). The GMPEs adopted for this work study are Atkinson and Boore (2006) and Toro et al. (1997), they are two famous models for SCR like Brazil.

The Atkinson and Boore (2006) model defined a ground-motion prediction equation for hard-rock sites based on a stochastic finite fault model for eastern North America (ENA). These equations are developed for response spectra, peak ground acceleration (PGA) and peak ground velocity (PGV) for hard sites in ENA. Besides that, Toro et al (1997) developed

ground motion attenuation equations for rock sites in central and eastern North America based also on the predictions of a stochastic ground motion model applicable for hard rocks.

Based on the fact that southeastern Brazil can be approximated to the seismicity found in eastern North America as both are characterized as stable continent regions, these two GMPEs models presented above will be used on R-CRISIS analysis for each seismic source zone model defined previously.

Reference	Magnitude Range	Distance Range (km)	Period Range (s)	Site classification v_{s30}
Atkinson and Boore (2006)	$M_w = 3.5 - 8.0$	$R_{rup} = 1 - 1000$	0.01 - 5.0 , PGA	2000m/s and 760m/s
Toro et al. (1997)	$M_w = 5.0 - 8.0$	$R_{JB} = 1 - 1000$	0.00 - 2.0, PGA	2800m/s

Table 14 - Description of the ground motion equations

The GMPEs for stable continental regions are usually derived for very hard rock sites with the shear wave travel time averaged soil shear-wave velocity of the upper 30m, v_{s30} , ranging between 2000 and 2900 m/s with the exception of Atkinson and Boore [2006] who provide GMPEs for $v_{s30}=760$ m/s. The distance range is the horizontal value of the shortest distance from a site to the fault rupture, R_{rup} , and the Joyner-Boore distance, R_{JB} .

3.4 TREATMENT OF UNCERTAINTIES IN PSHA

There are two types of uncertainties that exist in earthquake hazard analysis: aleatory and epistemic uncertainties. Aleatory uncertainty represents the natural randomness in a process, while epistemic uncertainty is the lack of knowledge introduced in a model that tries to represent an actual behavior.

In PSHA analysis, the standard deviation of GMPEs can be used to deal with aleatory uncertainty. Epistemic uncertainty can be addressed with a logic tree, in which weights are applied to the branches to reflect confidence in given options (Atkinson and Boore 2006; Toro et al. 1997). It should be noted that logic trees can be used to include different hypotheses in

PSHA as they are often used for altering recurrence rates of faults, geometry of seismic source zones, and characteristic magnitudes.

In this work study, the GMPEs proposed by Atkinson and Boore (2006) and Toro et al. (1997) are employed to calculate the earthquake hazard in terms PGA and SAs. To treat epistemic uncertainty, a logic tree is used, allocating weights for each case of seismic source zone model and weights of 0,6 and 0,4 to each branch for the GMPEs of Atkinson and Boore (2006) and Toro et al (1997), respectively. Higher weights are given to Atkinson and Boore (2006) equation because such model considers a magnitude range that better describe the working catalogue of this study. Seismic zone models 2 and 3 have higher weight because their division of the southeastern territory is more discretized, based on the fact that the GMPEs is directly influenced by shape of the source zone.

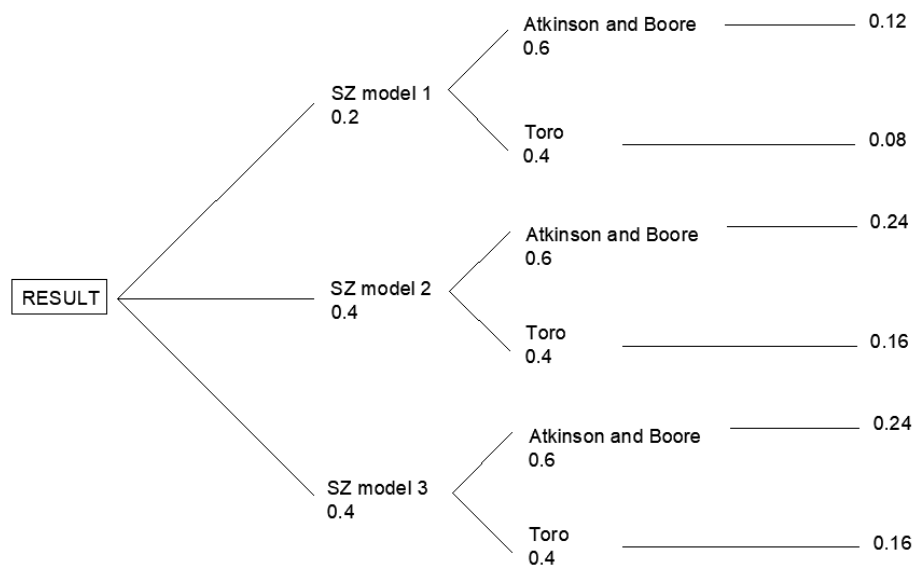


Figure 30 - Logic tree for the GMPEs chosen and each seismic zone model.

Finally, with all the parameters defined for each case of seismic source zone, the ground motion prediction equations selected and the logic tree with their weights, it will be possible to estimate the seismic hazard for southeastern Brazil using the software R-CRISIS.

4 R-CRISIS PROGRAM APPLICATION

The software R-CRISIS computes seismic hazard using a probabilistic analysis that considers earthquake occurrence probabilities, attenuation characteristics and geographical distribution of earthquakes. The earthquake occurrence can be modeled as a Poissonian process in the software with magnitude-frequency relation by the Gutenberg-Richter law. The source geometry is modeled as areas, lines or points. R-CRISIS admits three families of ground motion equations: attenuation tables furnished by the user, built-in parametric models and generalized attenuation models. The two GMPEs selected for this study, Atkinson and Boore (2006) and Toro et al (1997), are already defined in the software and can be selected directly during the input steps.

The software discretizes the source zones into elements of appropriate size, whose seismicity rate is redistributed proportionally to their size. For each discretized element the exceedance probability is evaluated. The probabilities for all magnitudes and sources are then accumulated in order to compute the overall exceedance probabilities.

The calculations are made for points of a grid that cover all the territory, with a separation of $0,1^\circ$ both in longitude and latitude. Results are obtained for PGA and SA (T) starting from $T = 0,01s$ up to $T = 2s$ and for return period of 475 years.

4.1 SOFTWARE INPUT

The first step for the probabilistic seismic hazard analysis with R-CRISIS is defining the data of the computation site. To define the site of Arraial do Cabo in the program is necessary to provide the name, the origin coordinates, the increment in degrees for orthogonal directions and the number of lines for the grid, because when hazard maps are required as output of the PSHA, the computation site needs to be defined in terms of a grid.

The next definitions are the source zones geometry data. The geometry model for this study is area source and the vertices coordinates must be provided as initial definition of the geometry. The depth of each vertex needs also to be provided and considering the stable continent region, the value of 25km is a reasonable choice.

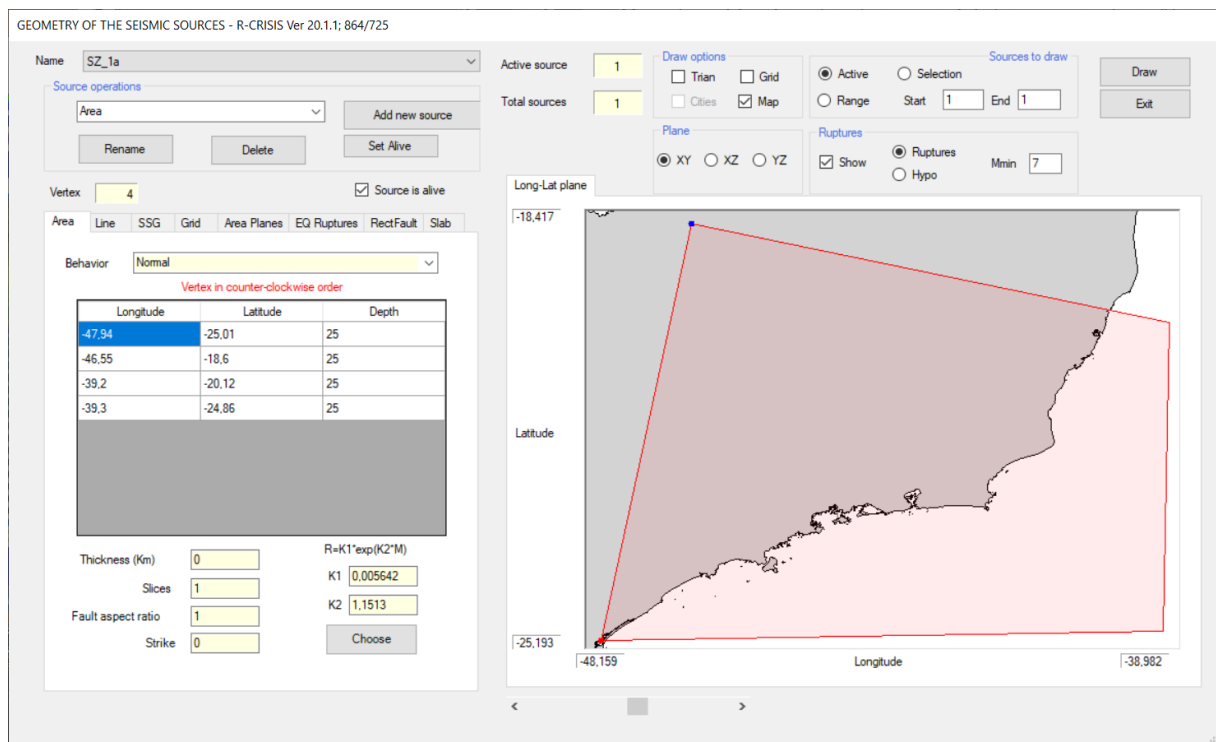


Figure 31 - Source zone geometry data as R-CRISIS input for the seismic source zone 1a

The Figure 31 shows the input for the seismic zone model 1a as an example. The same procedure is done for all the seismic zone models with their vertices already defined in the previous chapters of this study. In order to facilitate the verification of the location of the seismic sources, a reference map of the southeastern region of Brazil is uploaded. For the models that have more than one seismic source zone is possible to add a new source and provided its vertices as well. The depth of 25 km was considered for all the models. Besides that, the rupture parameters (K's) define the size of the rupture area and was provided by the built-in models of the program.

The next definition are the seismicity parameters. All the seismic sources zones in the R-CRISIS project need to be assigned seismicity parameters. This study is based on the Gutenberg-Richter law and must be assigned the threshold magnitude (M_0) for the selected source, the average annual number of earthquakes with equal or higher magnitude than M_0 , the b-value for the source, the coefficient of variation of the b-value, the number of magnitudes and the expected value of the maximum magnitude for the source.

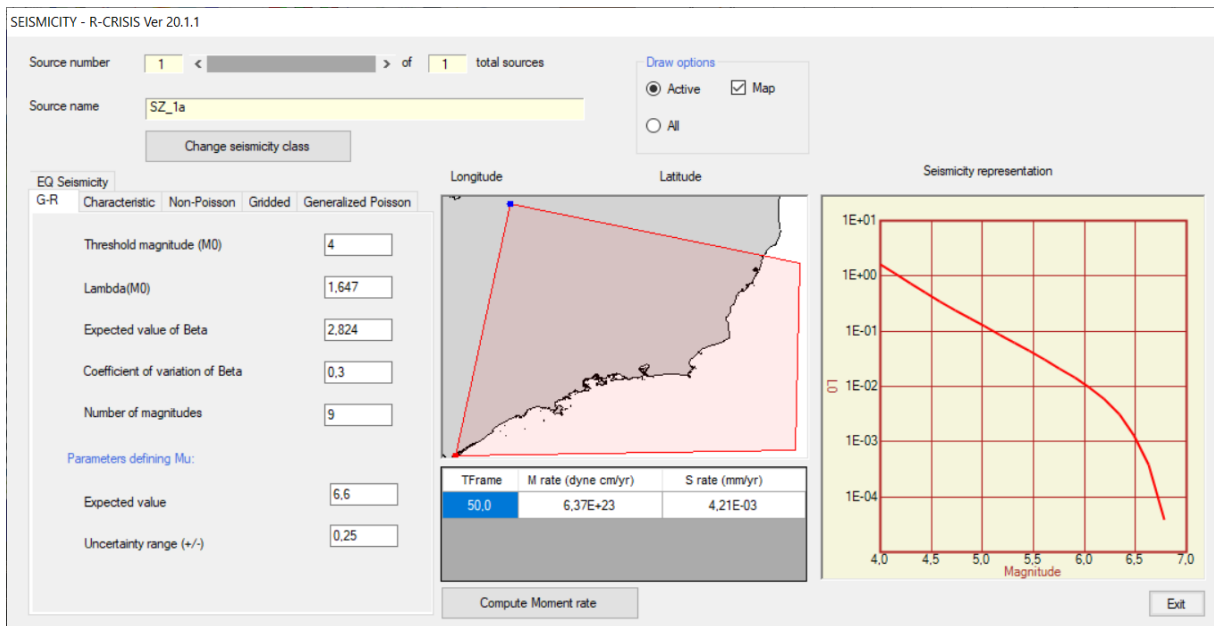


Figure 32 - Seismicity data input related to the seismic source zone model 1a

There are equal parameters for the three models of seismic source zones. The lower threshold magnitude is 4,0 as already defined considering the engineering significance of an earthquake occurrence. The coefficient of variation of b-value is defined in terms of the natural logarithm and this value is to consider the uncertainty in β . Based on the values found for each case of seismic source zone, the value of the coefficient of variation of β was calculated and it is 0,3. The number of magnitudes is related to the one used in the hazard integration process and is usually 9, smaller number for this parameter is rarely used.

Another parameter that is common to all the seismic source zones is the expected value of the maximum magnitude. The working catalog for this study has one event with the highest magnitude found and it is $M = 6,1$. Considering a possible range of $\pm 0,5$, the expected value of the maximum magnitude is $M_u = 6,6$. Finally, the last parameter is the uncertainty range, a number that indicates that the maximum magnitude will have a uniform probability density function, centered at its expected value. Based in other PSHA, the value of this uncertainty range is considered $\pm 0,25$ in this study.

SZ models	M0	ν_0 (M0)	β	Coef. Variation β	Number of Mag.	Mu	Range of Mu
SZ(1a)	4,0	1,647	2,824	0,3	9	6,6	0,25
SZ (2a)	4,0	1,257	2,928	0,3	9	6,6	0,25
SZ (2b)	4,0	0,426	2,358	0,3	9	6,6	0,25
SZ (3a)	4,0	0,702	2,983	0,3	9	6,6	0,25
SZ (3b)	4,0	0,532	2,936	0,3	9	6,6	0,25
SZ (3c)	4,0	0,426	2,358	0,3	9	6,6	0,25

Table 15 - Parameters of each seismic source zone for seismicity input of R-CRISIS

The fourth step of the input for the PSHA on R-CRISIS is the definition of the attenuation data. The two ground motion prediction equations for this study are Atkinson and Boore (2006) and Toro et al. (1997) and they are already defined as an option of attenuation data to the R-CRISIS project.

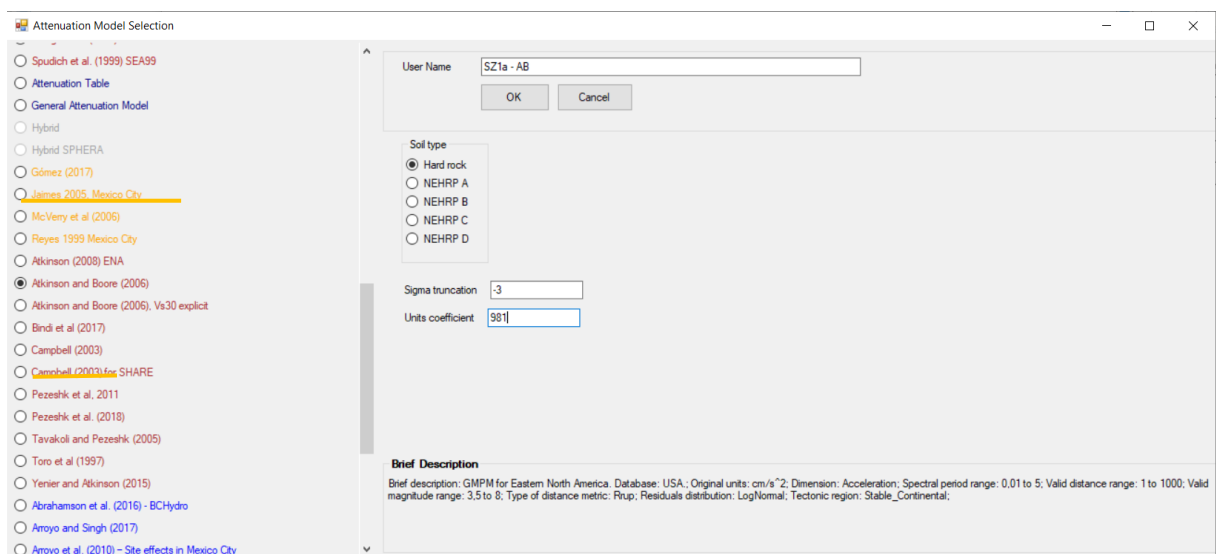


Figure 33 - Attenuation model selection for R-CRISIS input

The Figure 34 shows the selection of the Atkinson and Boore (2066) GMPE for the seismic source zone model 1a. The software gives a brief description of the GMPE in the bottom of the screen. The reference ground type for the southeastern Brazil is hard rock, the sigma truncation is the standard deviation as ground motion parameters are lognormally distributed. An overall description of the GMPE selection on R-CRISIS is shown in Figure 35. The same procedure is done when the analysis is done with Toro et al. (1997) attenuation equation.

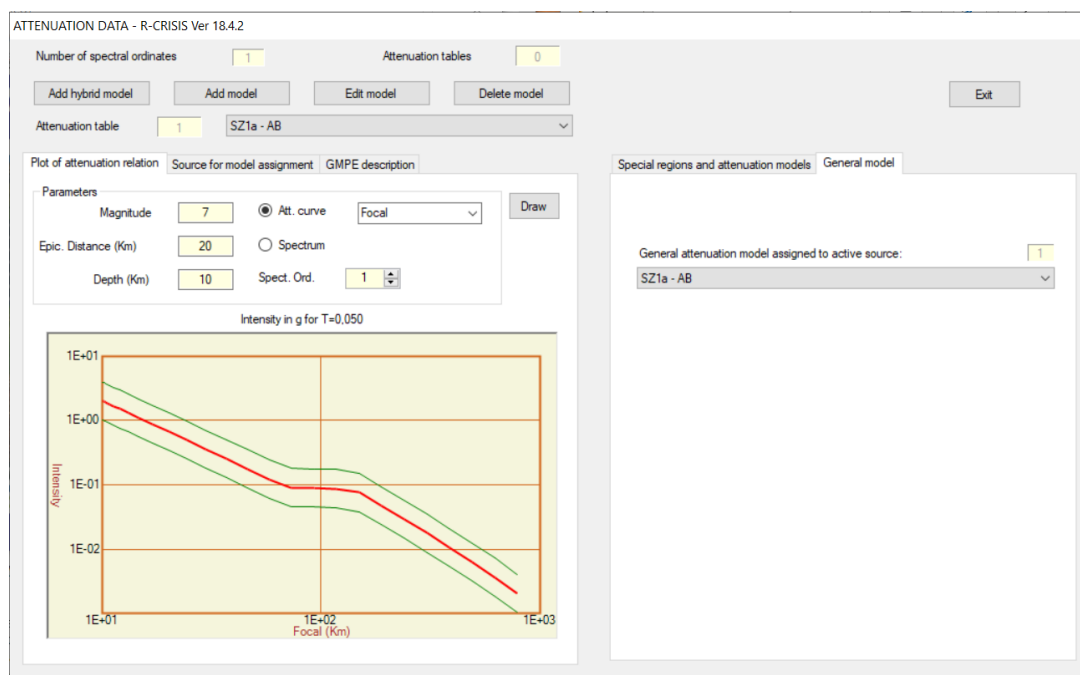


Figure 34 - Attenuation data input of R-CRISIS software

The next input are the spectral ordinates. It is necessary to define the number of spectral ordinates and their associated fundamental periods. For this study it was defined to use total number of 50 acceleration spectral ordinates, varying from the lower limit of 0.01g intensity level until upper limit of 2g intensity level. These limits are for the computation of the exceedance probabilities within the defined timeframe. The spacing type of the exceedance probability plot at each location is the logarithmic spacing between these intensity points. Besides that, all the spectral ordinates are defined in terms of the unit g.

INTENSITIES FOR EACH SPECTRAL ORDINATE - R-CRISIS Ver 20.1.1

Spectral ordinates

Total number of spectral ordinates: 50

Actual spectral ordinate: 1

Structural period of actual spectral ordinate: 0.01

Lower limit of intensity level: 0.01

Upper limit of intensity level: 2

Spacing

Log Linear PEER Large PEER

General values

Units: g

Number of levels of intensity for which seismic hazard will be computed: 50

Exit

Figure 35 - Intensities for each spectral ordinate for R-CRISIS input

Finally, the last data that must be defined to start the analysis are the global parameters. The reference of the structure lifetime, it means the time frame, is defined for 50 years. This study is considering a return period of 475 years, since the Brazilian Standard 15421 (NBR 15421) defines that the values to be defined as characteristic nominal for seismic actions are those with a 10% exceedance probability in the unfavorable direction, over a period of 50 years, which corresponds to a return period of 475 years. However, the R-CRISIS allows only the following possible return periods shown in Figure 36. Because of that, the approximation of a return period of 500 years is being considered.

GLOBAL PARAMETERS - R-CRISIS Ver 20.1.1

Integration parameters

Maximum integration distance km

Minimum triangle size km

Minimum Distance/Triangle Size ratio

CAV filter

Filter type

Time frame

Map return period (years)	PE in 50 years
100	3.93E-01
250	1.81E-01
500	9.52E-02
1000	4.88E-02
2500	1.98E-02

Figure 36 - Global parameters for the PSHA analysis

Considering a return period of 475 years ($T_r = 475$ years) and a reference lifetime structure of 50 years ($V_r = 50$ years), the probability that a critical event occurs in V_r years can be refined as the following equation.

$$T_r = \frac{-V_r}{\ln(1 - P_{VR})} \quad (19)$$

Applying the values defined before, the probability P_{VR} is 0,1.

These are the important steps for R-CRISIS input computations. After running the program for each one of the 6 analyses, the PSHA graphics results can be checked. The three models of seismic source zones defined in this study were analyzed in terms of the two GMPEs selected, Atkinson and Boore (2006) and Toro et al. (1997). Consequently, there are 6 graphics of 50-year exceedance rate curves for $T=0,01s$ and 6 graphics of uniform hazard acceleration response spectra for 0.10-in-50-year exceedance probability, it means, for a return period of 475 years, resulting from the indicated GMPEs.

4.2 R-CRISIS ANALYSIS RESULTS

In the following figures it will be possible to compare the results found for each of the total six analyses done. The logic tree was defined to capture the inherent uncertainty in the GMPEs. The city selected to present specific results is Arraial do Cabo, located in Rio de Janeiro state. This choice is justified by the fact that Arraial do Cabo is the easternmost city of the southeastern region, with important geographical location in relation to offshore activities. The following figures show the seismic hazard maps as R-CRISIS output for three of the seismic source zone models and each GMPE selected for these PSHAs. The reference site Arraial do Cabo is the central point of the 3x3 grid.

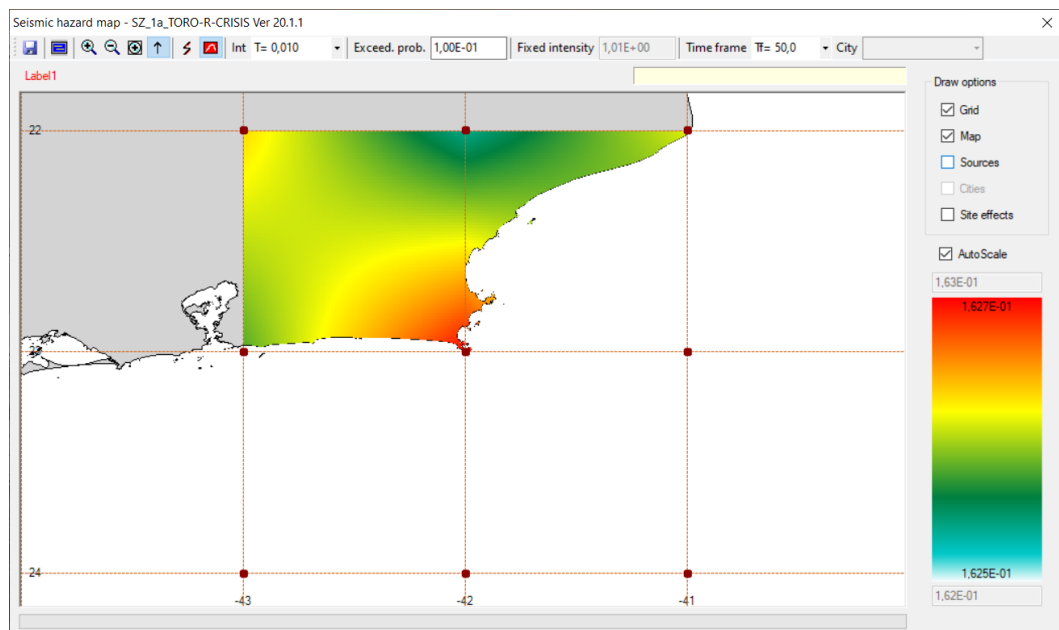


Figure 37 - Seismic Hazard Map for seismic source zone Model 1 using Toro et al. (1997) GMPE.

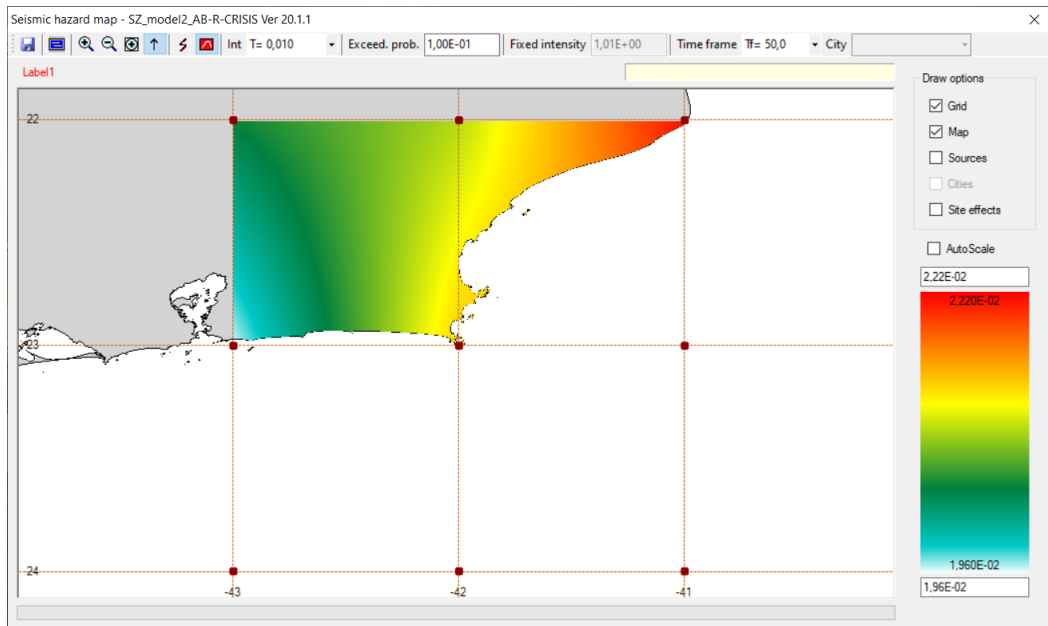


Figure 38 - Seismic Hazard Map for seismic source zone Model 2 using Atkinson and Boore (2006) GMPE

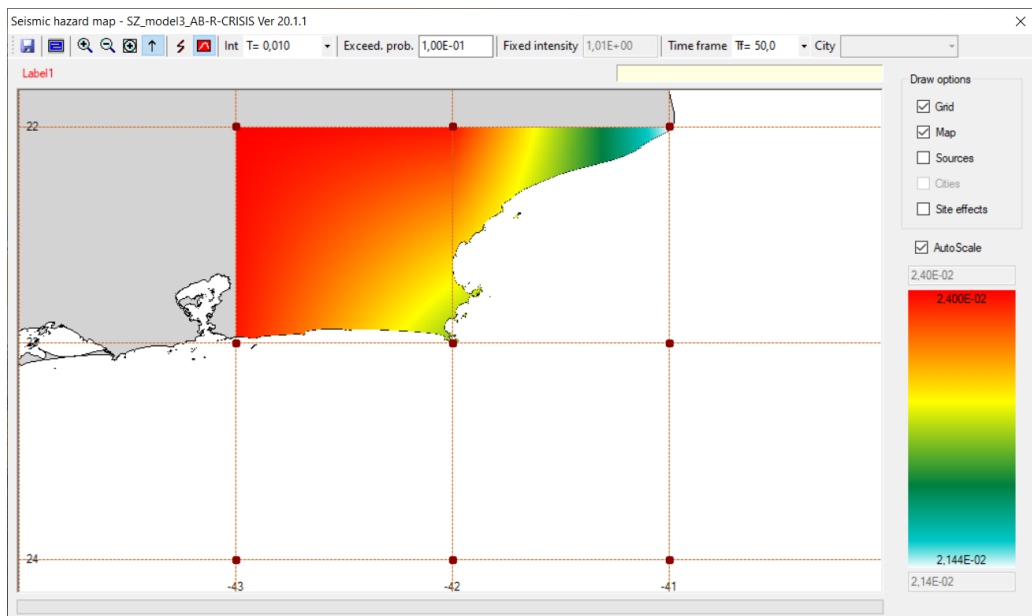


Figure 39 - Seismic Hazard Map for seismic source zone Model 3 using Atkinson and Boore (2006) GMPE

Southeastern Brazil has been analyzed before in terms of PSHA by Dourado (2013), Berrocal et al. (2013) and Assumpção et al. (1997) , and based on these studies, the common acceleration found is 0,025g for a return period of 475 years. Consequently, starting from the point of view that they are reliable studies, and considering that Atkinson and Boore (2006) is the GMPE that best describes the scenario for a PSHA analysis in southeastern Brazil, the seismic model with 3 source zones, Figure 39, is the best approximation. The seismic source zone model 3 using Atkinson and Boore (2006) equations results in an approximated acceleration of 0,022g.

The next figures below show graphics with the 6 analyses done in terms of exceedance curves with probability in 50 years and the response spectra with periods in seconds and the acceleration intensity in g.

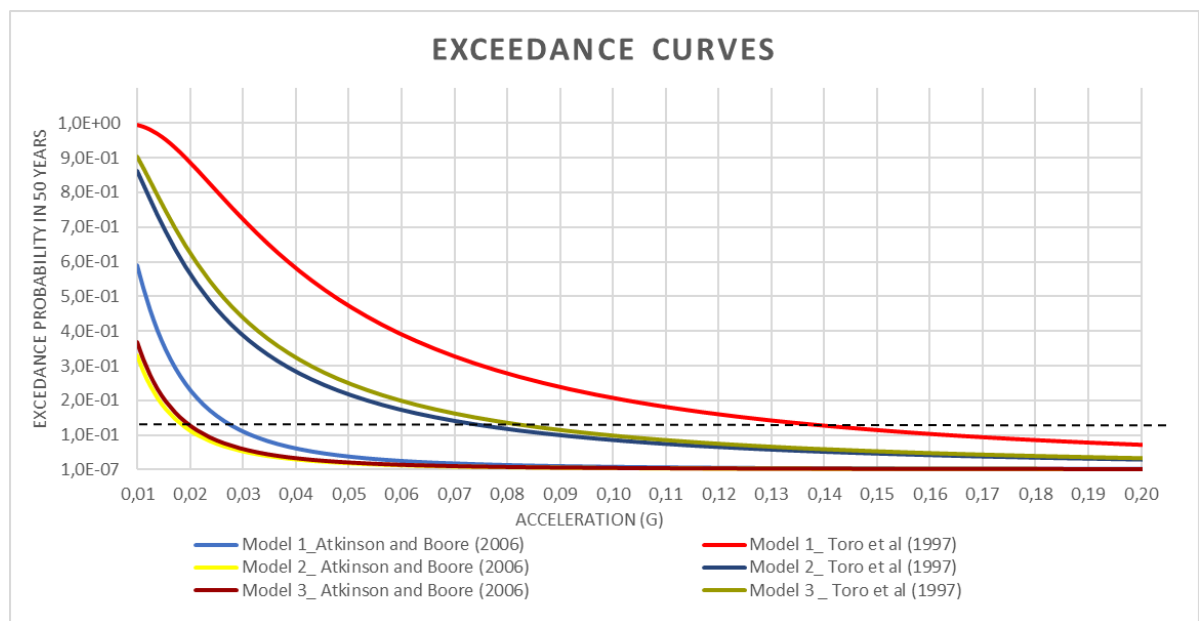


Figure 40 - 50-years exceedance rate curves for $T=0.01s$ S_a spectrum ordinates contributed by different seismic source zone models and GMPEs

The results illustrate that, for PSHA done with the GMPE of Atkinson and Boore (2006), the exceedance probability in 50 years, considering an acceleration of 0,02g , i.e. a substantially lower value than when GMPE of Toro et al. (1997) is used. These lower values are expected since, for stable continent regions like Brazil, the exceedance probability of a seismic event is definitely low, and this can be compared to previous studies.

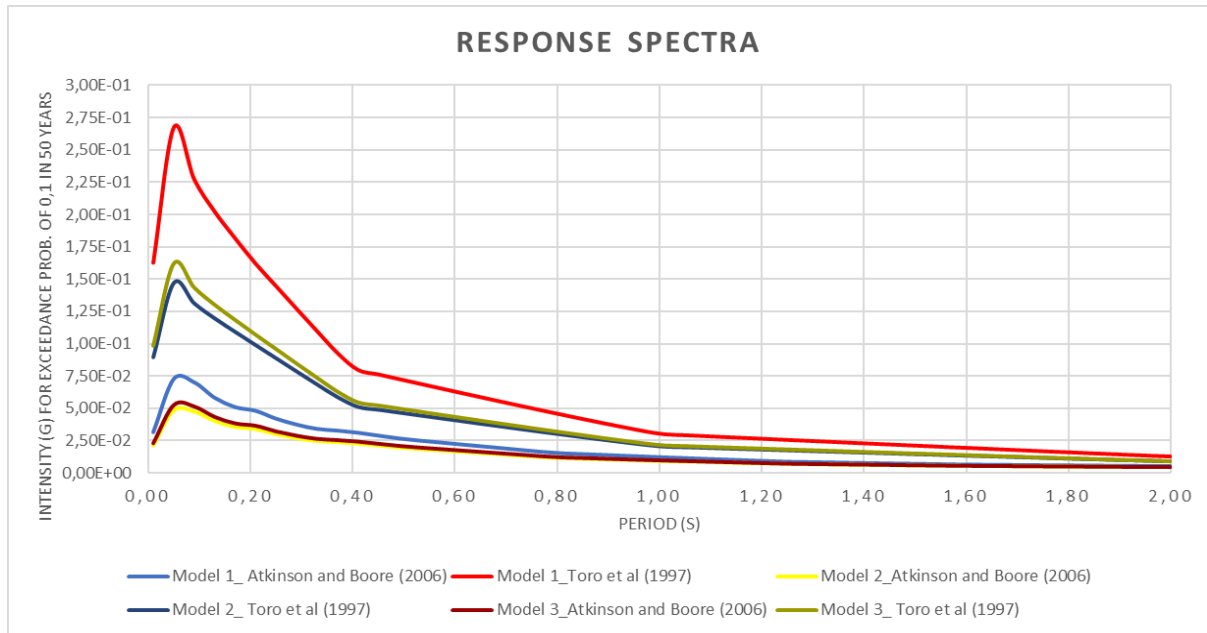


Figure 41 - Uniform Hazard acceleration response spectra for 0.10-in-50 year exceedance probability for each seismic source model and GMPEs selected

The response spectra are important R-CRISIS outputs in order to have a better engineering grasp of the implications of each analysis done. It is notable that for all the analyses done with the GMPE of Toro et al. (1997) the values are considerably higher. This may be explained by the fact that this equation has a valid magnitude range from 5,0 to 8,0, really high values for a SCR like southeastern Brazil which has a working catalog with events starting from $M_w = 2,6$. Besides that, the type of distance metric is the Joyner and Boore distance (RJB). In contrast, the Atkinson and Boore (2006) is an improved model for stable continents with a valid magnitude range from 3,5 to 8,0 and the fault distance or rupture distance (Rrup) as the type of distance metric.

The attenuation equation is directly related to the shape of the seismic zones and the source-to-site distances, it means the distance metric. Consequently, the model 3 defined in this study with 3 seismic source zones has a more discretized solution, because the continental shelf, the coastal part and Minas Gerais state have different behaviors, based on the working catalog. That is the reason why the third seismic source model defines these three zones.

It is difficult to have the perfect seismic scenario characteristics of Brazil without a specific GMPE for the country. Therefore, the use of these two GMPEs is to have the best approximation of the reality and comparing with previous studies. This study found that, considering the model with 3 seismic source zones and a PSHA done with Atkinson and Boore (2006) as attenuation equation, the result is the most reliable one.

5 STRUCTURE EXAMPLE APPLICATION

The first part of this work was making a probabilistic seismic hazard analysis on a site in southeastern Brazil with R-CRISIS program in order to get the acceleration response spectrum. The logic tree approach was applied to the treat epistemic uncertainties of a PSHA, weights were defined for each case of seismic source zone model and weights of 0,6 and 0,4 to each branch for the GMPEs of Atkinson and Boore (2006) and Toro et al (1997), respectively. The logic tree analysis was done with R-CRISIS program and an acceleration response spectrum was computed for returns periods of 475 years and 2475 years.

The proposal now is applying this acceleration response spectrum in a theoretical concrete building structure as a dynamic loading for a structural analysis with the program ROBOT, an Autodesk software. The aim of this structural analysis is getting the stresses of a central column caused by the self-weight of the building and the seismic acceleration with a return period of 475 years and 2475 years, this last one based on the guidelines of the Brazilian Standard – NBR 15421. The goal of this analysis in to show the values for bending moments and displacements of this column.

In addition, a second structural analysis will be computed considering, this time, the self-weight of the building and a wind force, as a static loading. Furthermore, values for bending moments and displacements of the same column will be made.

In Brazil is not common to consider seismic dynamic forces in residential or commercial buildings. Therefore, the goal of these two analyses is to compare the stresses and displacements found for each loading situation and discuss the critical scenario that may happen with a potential seismic event occurrence in comparison with the scenario with only wind forces acting. Both wind and seismic events, among the environmental actions on civil structures, present an important destructive potential, being responsible for a lot of material loss, and, in some cases, for the loss of human life.

The next sections will present the spatial model of the building applied into ROBOT software. The three analyses defined in the previous paragraph are the three separate inputs in the program, one considering the wind force in y+ direction, another one with the acceleration response spectrum with return period of 475 years and the last one with the return period of 2475 years. Following this, the results will be discussed based on the bending moment and the displacements of a central column of the building.

5.1 PRESENTATION OF THE SPATIAL MODEL

The concrete structure is an 8 storey residential building. In this case, it is a system with multiple degrees of freedom, which makes essential the use of a computational software to define the structure response under dynamic and static loadings. A 3D model is used with 336 bars elements and 4913 structural nodes. The columns were fixed at their bases to simulate reinforced concrete foundation blocks.

In order to complete the model of the building, we considered the generic self-weight load given directly by the software, linear masonry wall loads defined in the Brazilian standard - NBR 6120 - of 2,25 kN/m², wall cladding loads of 1,00 kN/m² and usage and occupancy loads also defined in NBR 6120 of 1,5 kN/m² for dormitories and 2,00 kN/m² for laundry and service areas.

The results will be analyzed with reference to a central column of the building, the column P11. The loading cases defined for the analysis have the wind and the seismic loads as primary actions. The values found for bending moment and displacements of this column under wind force and dynamics seismic forces will be discussed.

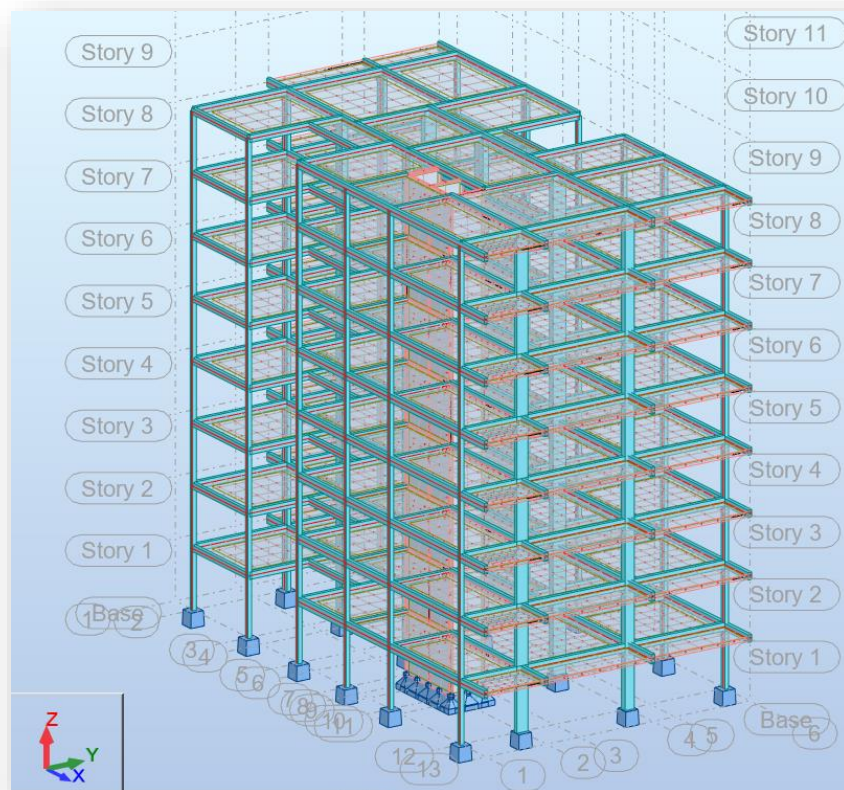


Figure 42 - 3D model of the concrete building in ROBOT software

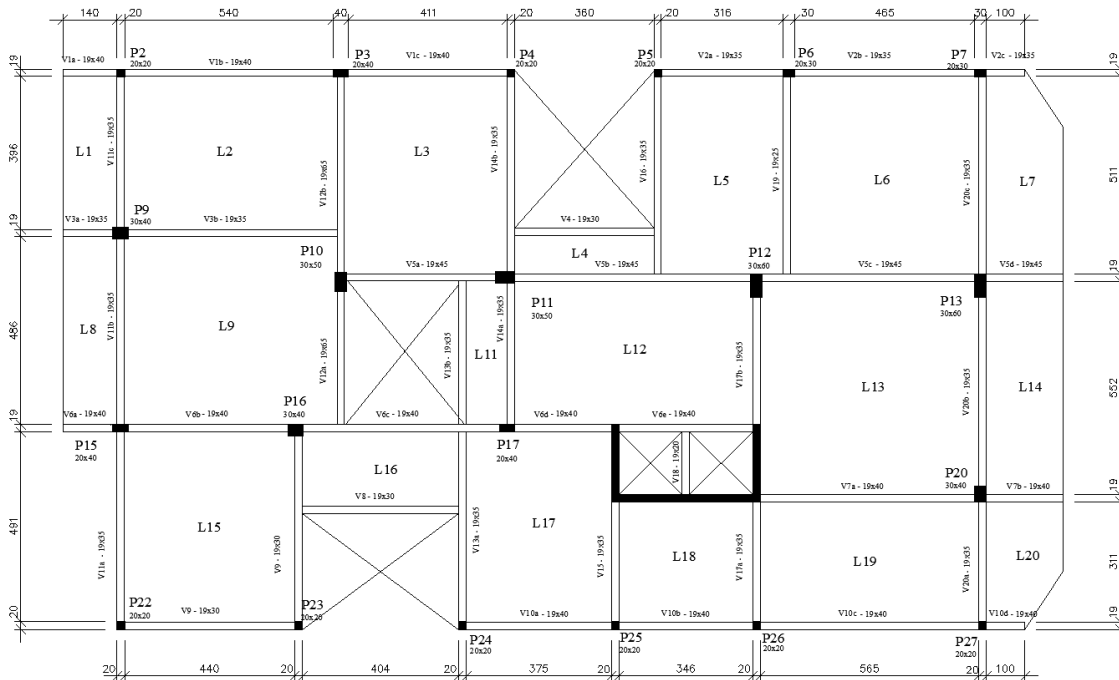


Figure 43 – Plan of the fifth storey of the building

The first analysis that will be carried out is the one considering only the self-weight, the usage and occupancy loads and the wind force as a static loading. The location of this example of structure is in the site of Arraial do Cabo city, the same used for the probabilistic seismic hazard analysis. Then, following the Brazilian Standard about wind forces in buildings (NBR 6123), is possible to determine the force caused by the wind in kN/m^2 based on basic wind speed, roughness of the terrain, dimensions of the building and statistics factors. Therefore, it was applied in the 3D model a static loading of $1,5\text{kN/m}^2$ in y-y direction of the building, the side of the largest building façade to quantify the wind forces. The results will be presented in the following section.

The seismic analysis of a structure is the response analysis of this building when it is required by a movement in the base acted by a seismic event. It was considered two cases of seismic analyses through the acceleration response spectra for 475 years and 2475 years determined though the logic tree analysis. The accelerations were applied in a horizontal direction that corresponds to the model direction $y+$, the same considered for the wind action.

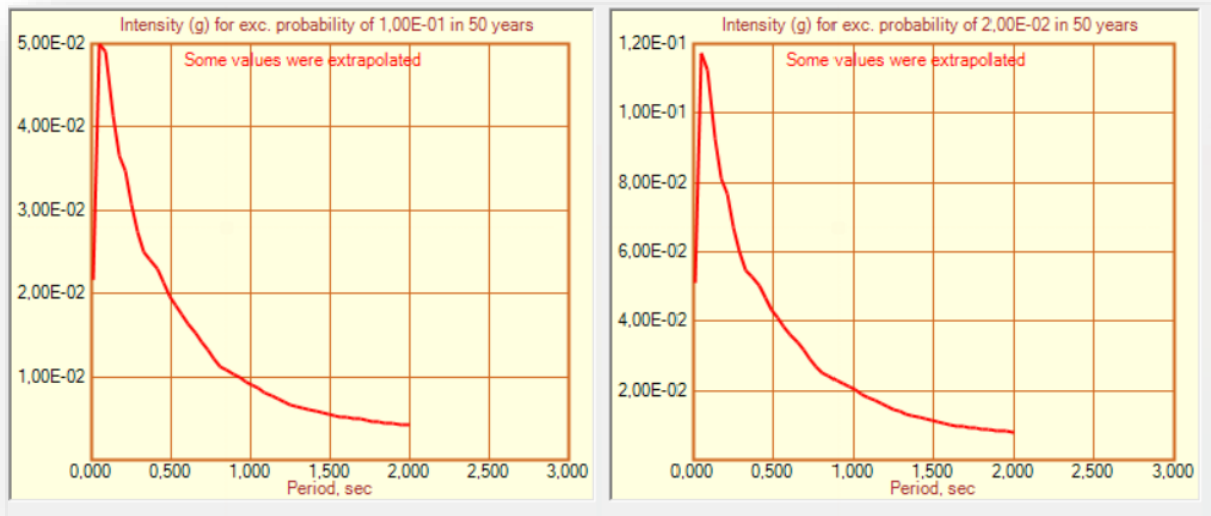


Figure 44 - Acceleration response spectrum for 475 years (left); Acceleration response spectrum for 2475 years (right).

5.2 RESULTS ANALYSIS

The input data was defined for ROBOT software and the three analyses results could be checked. According to the table 16, it can be noticed that bending moment reaction in y direction at the base of the column P11 is higher when a wind loading is considered than when a seismic event occurs for a return period of 475 years. This is a reasonable result as the building is in a stable continent region and the wind force is a much more significant force than a seismic event with acceleration of 0,0215g. This acceleration action when compared with the wind force has lower structural response effect.

Bending Moment at the column P11 base (kNm)		
Wind	Sismo Tr=475years	Sismo 2475years
316,40	165,31	413,92

Table 16 - Bending moments values at the base of the column P11 in Y direction.

However, when the response spectrum for 2475 years return period is considered, there is a different scenario, the peak acceleration now is 0,0509g. This seismic event presents a higher bending moment reaction at the base of the column P11. It can be explained by the fact that the accelerations are two times higher than before and consequently, this seismic event is stronger than a wind occurrence.

In relation to the displacements of the structure on each storey, analyzing the results after running the software, it can be concluded that for an 8 storey building, displacements are high and cannot be disregarded when a seismic event for a return period of 2475 years is considered.

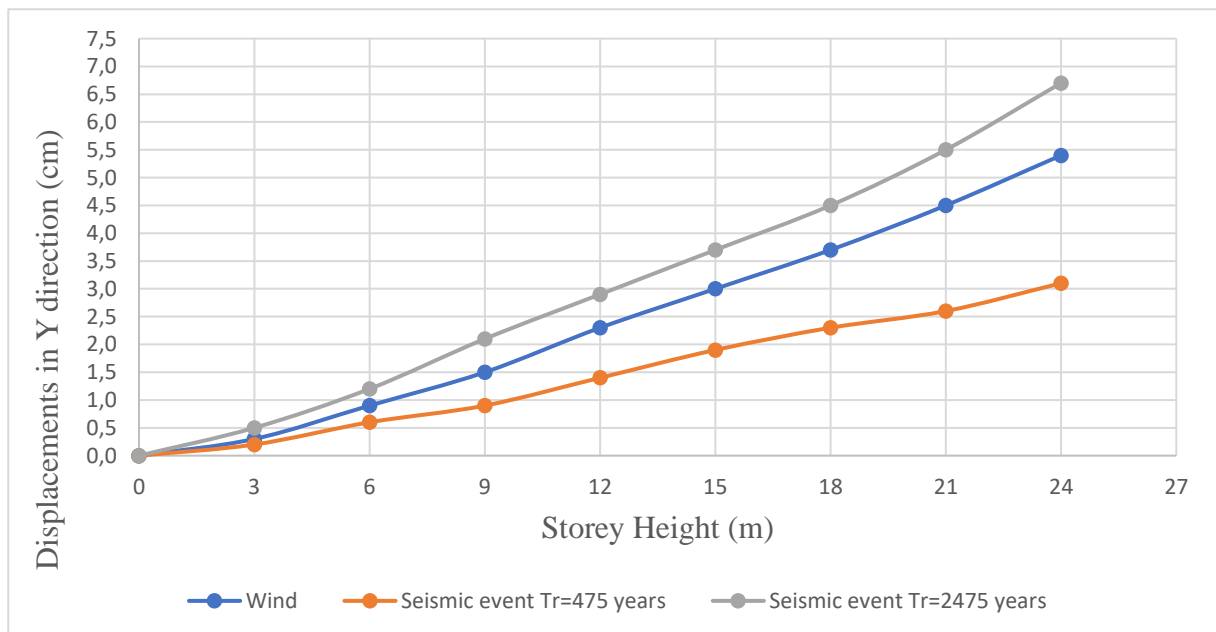


Figure 45 - Displacements along the height of the building in Y Direction

On the top of the column P11, at 24 meters from the building base, it can be noticed that the wind action can cause a displacement around 5,4cm while a seismic event with a return period of 2475 years there is a considerable displacement of 6,7cm and with a return period of 475 years the value can reach almost 3,1cm.

Based on these results, even if the probability of occurrence of an earthquake in southeastern Brazil is low, a seismic event with a return period of 2475 years will cause unexpected damages. This is an important analysis to show how considerable a seismic event should be when a structural design is being done. Even if seismic analysis is not mandatory for residential and commercial building in southeastern Brazil, these results from ROBOT software show that seismic events can also cause damages and losses when compared with the wind action. The probability of occurrence is low but is not null and would be impactful.

6 CONCLUSIONS

A site specific probabilistic seismic hazard analysis has been performed for the city of Arraial do Cabo, located in the seismically calm region of Southeastern Brazil. The study was undertaken to achieve response spectra results with R-CRISIS program and compare with previous studies. This software is worldwide recommended for seismic hazard analysis specially in active seismic continental regions, therefore reliable results were expected when stable seismic region is been analyzed.

Unfortunately, the limited earthquake catalogue for the entire country and the lack of strong motion recordings inevitably means that there was considerably epistemic uncertainty in both seismic source and ground-motion characterization models. These uncertainties were captured through a logic-tree formulation with six branches, each one for different seismic source zones geometry and the selected ground motion prediction equations. The weights for each branch analysis of the logic-tree were defined based on how much each of the two GMPEs would represent the seismicity scenario of southeastern Brazil.

The results show that the generated hazard maps compare well with results from recent PSHA studies. The peak ground acceleration of 0,022g found for the third seismic source zone model, the most discretized one with reason to the region of the site, based on the ground motion prediction equation of Atkinson and Boore (2006) is what was expected, confirming the reliability of the analysis with R-CRISIS software.

The purpose of the deterministic analysis in a practical structural analysis in a reinforced concrete structure was to quantify in numbers the stresses caused by a seismic event in an ordinary residential building in southeastern Brazil. Concerning to have a starting point for comparing results, the wind loading was included, as this is a mandatory loading to be considered in a structural analysis, especially in coastal cities like Arraial do Cabo. Consequently, it became notable that a seismic event with a return period of 2475 years would cause greater bending moments reactions and nodes displacements in a structure.

Besides the fact that Brazil is a seismic stable region and the return period of 2475 years of the acceleration response spectrum analyzed is vast, the results show that probabilities are not null at all and as well as economic losses can happen, life losses must be considerable also. There is consequently strong motivation to invest in seismic hazard studies in Brazil. This study results may have different applications and can serve as input for future seismic risk studies and structural analyses considerations.

REFERENCES

ALMEIDA, A. A. D. et al. Probabilistic seismic hazard analysis for a nuclear power plant site in southeast Brazil. **Journal of Seismology**, v. 23, n. 1, 2019

ASSOCIAÇÃO BRASILEIRA DE NORMAS TÉCNICAS. NBR 6123: Forças devidas ao vento em edificações. **Associação Brasileira de Normas Técnicas**, p. 66, 1988. (in Portuguese)

ASSOCIAÇÃO BRASILEIRA DE NORMAS TÉCNICAS. NBR 15421: Projeto de estruturas resistentes a sismos – Procedimento. **Associação Brasileira de Normas Técnicas**, Rio de Janeiro, 2006. (in Portuguese).

ASSUMPÇÃO, M. et al. The São Vicente earthquake of 2008 April and seismicity in the continental shelf off SE Brazil: Further evidence for flexural stresses. **Geophysical Journal International**, v. 187, n. 3, p. 1076–1088, 2011.

ASSUMPÇÃO, M. et al. Intraplate seismicity in SE Brazil: Stress concentration in lithospheric thin spots. **Geophysical Journal International**, v. 159, n. 1, p. 390–399, 2004.

ASSUMPÇÃO, M.; SACEK, V. Intra-plate seismicity and flexural stresses in central Brazil. **Geophysical Research Letters**, v. 40, n. 3, p. 487–491, 2013.

ATKINSON, G. M.; BOORE, D. M. Earthquake ground-motion prediction equations for eastern North America. **Bulletin of the Seismological Society of America**, v. 96, n. 6, p. 2181–2205, 2006.

BERROCAL, J.; ROMERO, T.; RONDÁN, E. R. Probabilistic Assessment of Seismic Hazard in Southeastern Region of Brazil. p. 1694–1698, 2014.

BHATTI, A. Q. et al. Probabilistic seismic hazard analysis of Islamabad, Pakistan. **Journal of Asian Earth Sciences**, v. 42, n. 3, p. 468–478, 2011.

DE ALMEIDA, A. A. D. et al. Probabilistic seismic hazard analysis for a nuclear power plant site in southeast Brazil. **Journal of Seismology**, v. 23, n. 1, 2019

DOURADO, J. C. Mapa de Ameaça Sísmica na Plataforma Continental do Sul/Sudeste. p. 1730–1733, 2014. (In Portuguese).

FACCIOLI, E. Recent evolution and challenges in the Seismic Hazard Analysis of the Po Plain region, Northern Italy: The second Prof. Nicholas Ambraseys distinguished lecture. **Bulletin of Earthquake Engineering**, v. 11, n. 1, p. 5–33, 2013.

FERNANDEZ ARES, A.; FATEHI, A. Development of probabilistic seismic hazard analysis for international sites, challenges and guidelines. **Nuclear Engineering and Design**, v. 259, p. 222–229, 1970.

FOURIER, U. J.; COTTON, F. Seismic Hazard Harmonization in Europe Project Acronym : SHARE Deliverable 4 . 2 : Regionally adjusted Ground Motion Prediction Equations (GMPE) for **Europe St** . n. 226967, 2010.

JAISWAL, K., PETERSEN, M., HARMSSEN, S., SMOCZYK, G. Assessing the Seismic Risk Potential of South America. **Second European Conference on Earthquake Engineering and Seismology**, p. 1–13, 2014.

JAISWAL, K.; WALD, D. An empirical model for Global Earthquake fatality estimation. **Earthquake Spectra**, v. 26, n. 4, p. 1017–1037, 2010.

JOHNSTON, A. C. Seismic moment assessment of earthquakes in stable continental regions - III. New Madrid 1811-1812, Charleston 1886 and Lisbon 1755. **Geophysical Journal International**, v. 126, n. 2, p. 314–344, 1996.

KROPIVNITSKAYA, Y. et al. A pipelining implementation for high resolution seismic hazard maps production. **Procedia Computer Science**, v. 51, n. 1, p. 1473–1482, 2015.

MCGUIRE, R. K.; ARABASZ, W. J. 12. An Introduction to Probabilistic Seismic Hazard Analysis. **Geotechnical and Environmental Geophysics**, p. 333–354, 1990.

NOBREGA, P. G. B.; NOBREGA, S. H. S. Perigo Sísmico No Brasil E a Responsabilidade Da Engenharia De Estruturas. **Holos**, v. 4, p. 162, 2016. (in Portuguese).

ORDAZ, M. et al. CRISIS2008: A flexible tool to perform probabilistic seismic hazard assessment. **Seismological Research Letters**, v. 84, n. 3, p. 495–504, 2013.

PARRA, H.; BENITO, M. B.; GASPAR-ESCRIBANO, J. M. **Seismic hazard assessment in continental Ecuador**. [s.l.] Springer Netherlands, 2016. v. 14

PETERSEN, M. D. et al. Sensitivity study of seismic hazard and risk for the continent of South America. **16th World Conference on Earthquake Engineering**, p. Paper Nr 456, 2017.

PETERSEN, M. D. et al. Seismic hazard, risk, and design for south america. **Bulletin of the Seismological Society of America**, v. 108, n. 2, p. 781–800, 2018.

ROCHA, M. P. et al. Causes of intraplate seismicity in central Brazil from travel time seismic tomography. **Tectonophysics**, v. 680, p. 1–7, 2016.

SALGADO-GÁLVEZ, M. A. et al. Probabilistic Seismic Risk Assessment in Manizales, Colombia: Quantifying Losses for Insurance Purposes. **International Journal of Disaster Risk Science**, v. 8, n. 3, p. 296–307, 2017.

SIANKO, I. et al. **A practical probabilistic earthquake hazard analysis tool: case study Marmara region**. [s.l.] Springer Netherlands, 2020. v. 18

SANTOS, S. H. C. et al. The New Brazilian Standard for Seismic Design. **World Conference on Earthquake Engineering**, n. 1999, 2008.

SANTOS, S. H. C. NBR15421- Projeto de Estruturas Resistentes a Sismos Estruturas de Edifício. [s.d.]. (in Portuguese)

SILVA, F. C. M. **Avaliação Do Risco Sísmico Nas Regiões Nordeste E Sudeste Do Brasil**. 2009, UFRJ, Rio de Janeiro. (in Portuguese)

SOUZA, F. S. DE et al. Quantificação da ação do vento em edificações – Comparação entre as metodologias da NBR-6123 e ASCE 7-05. **Introdução Dentre** as. n. 1, 2009. (in Portuguese)

WAHRHAFTIG, A. DE M. Ação do vento segundo a NBR 6123/88. **Ação do Vento**, p. 163–184, 2017. (in Portuguese)